Soils and Rocks
An International Journal of Geotechnical and Geoenvironmental Engineering
www.soilsandrocks.com
ISSN 1980-9743
ISSN-e 2675-5475

The 10th James K. Mitchell Lecture – In situ and lab tests work together to reduce uncertainties in TSF fragility assessment: a benchmark case-history

António Viana da Fonseca[1#]

Lecture

Keywords
Advanced laboratory tests
Iron tailings
Critical state parameter
Brumadinho B1 dam failure
Instability
Liquefaction

Abstract

This article, a written contribution of the 10th James K. Mitchell, delivered in Bologna on June, 10, 2022, describes the experimental characterisation of Brumadinho B1 tailings dam, that allowed to study analytically a unique case history, of a massive earthwork which suddenly failed on January 25th of 2019 in Minas Gerais (Brazil). This detailed characterisation comprised an advanced experimental programme using reconstituted and undisturbed samples recoiled in three sampling campaigns in the remaining post-morten dam/reservoir tailings, where the failure mechanism developed. The results that embrace evaluations of the physical, hydraulic, and mechanical properties, allowed to define the geotechnical parameters necessary for the referred analyses. This cannot be completed without knowing how to deal with a heterogeneous distribution of types of tailings generated from distinct iron rock masses in the mine, which was pursued with re-interpretation of in situ tests, some recent with high quality data, clustering in zones that could be discretized by overall types of soils with proper index behaviour and state conditions. The necessary parameters for constitutive models based on Critical State Soil Mechanics with Instability Locus that could be used in stability numerical simulations, will be discussed – in their conditions - that can define a reliable back calculation of the failure.

1. Prelude: The James K. Mitchell lecture series

In September 2004, in ISC'2 Porto, the heritage lecture in honour of the late Professor James K. Mitchell has started to be delivered by researchers and professional who have done important contributions in the area of in situ testing and geotechnical site characterization. During his residencies as a faculty member at the University of California-Berkeley and Virginia Polytechnic & State University, Professor Mitchell spearheaded several important research studies and produced many useful publications on the topics of in situ testing, specifically related to cone penetration testing, calibration chambers, vane shear testing, the interpretation of test measurements, soil liquefaction evaluation and geoenvironmental site assessment. To pay homage to his significant accomplishments, the TC 102 (former TC16) membership thought an invited lecture and keynote paper established in his name (The James K. Mitchell Lecture) would be an appropriate means to make this honor, as well as to recognize an upcoming and outstanding geotechnical engineer who has made recent contributions in the area of in situ testing. Towards the validity of this award, he was contacted and sought his advice and permission which were subsequently given. Based on the above impetus, TC 102 has awarded 10 invitations for the period of 2004 to 2022 for "The James K. Mitchell Lecture" to the following individuals:

- (2004) Hai-Sui Yu, Univ. of Nottingham, UK - ISC-2, Porto, Portugal
- (2006) Paul W. Mayne, Georgia Inst. Technology, USA - GeoShanghai, China
- (2008) Dick Campanella, Univ. British Columbia - ISC-3, Taipei, Taiwan
- (2010) Tom Lunne, Norwegian Geotechnical Inst., Norway - CPT'10, Huntington Beach, California

#Corresponding author. E-mail address: viana@fe.up.pt
[1]Universidade do Porto, Faculdade de Engenharia, CONSTRUCT-GEO, Porto, Portugal.

Submitted on July 29, 2025; Final Acceptance on November 13, 2025; Discussion open until August 31, 2026.
Editor: Renato P. Cunha
https://doi.org/10.28927/SR.2026.011425

- (2012) Peter K. Robertson, Gregg Drilling, USA - ISC-4, Las Vegas, Nevada, USA
- (2014) Mike Jamiolkowski, Studio Geotecnica, Italy - CPT'14, Perth, Australia
- (2016) An-Bin Huang, National Chiao Tung University, Taiwan - ISC-5, Brisbane/Gold Coast, Australia
- (2017) J.M. Powell, GeoLabs Ltd. - 19th ICSMGE, Seoul'2017
- (2021) Fernando Schnaid, UFRGS, Brazil - ISC6, Budapest 2021
- (2022) António Viana da Fonseca, FEUP, Portugal CPT'22, Bologna 2022

The lecture papers may be found in the applicable proceedings to the conferences listed above where the lectures have been presented. In addition, by special permission, the first four keynote papers labelled: The James K. Mitchell Lectures were printed in Geomechanics and GeoEngineering: An International Journal and in time other journals have accepted to make it.

The selection process is handled by nomination of viable candidates by official members, core members, advisors, and friends of TC 102 (former TC16). Approximately 2 years prior to the delivery of the lecture, the TC Chair and Secretary initiated the request for nominees via email notification and/or our website: www.webforum.com/tc102. Nominees are then voted on by the membership, usually within a one-month period. The chosen individual is invited to prepare a keynote lecture and a paper to be presented at an upcoming technical conference or symposium which has either a theme or sessions focused on the topic of in situ testing.

2. Introduction

2.1 Critical states and instability

Recent catastrophic failures of Tailings Storage Facilities (TSF), such as the Fundão, 2015, and Brumadinho, 2019, dams killed hundreds of people and are considered the largest environmental disaster in Brazil, highlighting the need for an improved understanding of the engineering properties of tailings and industrial waste materials. The susceptibility to cyclic mobility and liquefaction has been dealt obliquely with bias empiricism, lacking systematized theoretical background. A variety of hazard factors, dramatically increase the vulnerability of these structures, such as: (i) Rapid static loading (construction or tailings deposition); (ii) rapid cyclic loading (earthquakes, blasting or other vibratory actions); (iii) reduction of confinement (by sudden increases in water levels in the soil, by uncontrolled excavations in reservoirs or settlements of the foundations of natural massifs or dam retaining structures laying on loose submerged tailings; through interlayers created in deposition in liquid or compacted layers; (v) Internal erosion and/or piping through interlayers created in deposition in liquid or compacted layers; (vi) human interaction (drilling boreholes for installation of drainage or monitoring systems); (vii) localized loss of strength due to inflow from underground springs; (viii) loss of suction and strength in unsaturated zones above the water level; (ix) long term internal creep and relaxation (strains that develop with time under constant or long term repeated loads); and, others unknown to be faced in the future. A large number of these facilities are immobilized and have to be removed (decommissioned) due to the high levels of failure probability (last year the IR was involved in the risk assessment of more than fifty of these dams in Minas Gerais, Brazil, and around 50% were considered critical). This condition demands for particularly sensitive deconstruction techniques that require a very accurate knowledge of the consequences of the necessary interventions in terms of transient, static and vibrating loading and unloading on these highly unstable materials.

Due to the complexity of these actions and the sensitivity of these non-conventional waste materials, the engineering approaches to construct or deconstruct these TSF have to be sustained in reliable stability analyses based on powerful numerical codes with broad capacities in terms of effective stress-strain analyses with hydraulic coupling, based on complex constitutive models.

The susceptibility to cyclic mobility and liquefaction has already been identified yet not systematized. Using in situ and laboratory databases of reference projects in sandy, silty or even non-plastic sandy-silt materials, may contribute to the evaluation of their sensitivity to liquefaction.

Critical state concepts are more adapted for this purpose, and the optimization of the experimental works has been improving, both recurring to the most adequate in situ testing procedures and sampling techniques, as well as advanced laboratory tests (not necessarily the most complicated). The definition of the representative hydraulic and geotechnical parameters and the distribution in ponds and crests, have to be prioritized, seeking for the best engineering approaches and looking for safe solutions. The critical state line provides a robust framework for the characterization of mining tailings. Recent experimental data for non-plastic tailings and a large database for tailings and non-plastic fine soils show that the critical state parameters for non-plastic tailings follow the same trends as non-plastic soils as a function of particle-scale characteristics and very high void ratios as a result of liquid deposition (Morgenstern, 2018). Critical state lines determined for extreme tailings gradations underestimate the range of critical state parameters that may be encountered in a tailings dam; in fact, mixtures with intermediate fines content exhibit the densest granular packing at critical state (Hight, 2024).

The concepts of critical states have been complemented with laws of instability for these fragile soils (that is, with very high peak and residual resistance ratios). The optimization of the experimental work has to be done using in situ testing procedures, particularly the static piezocone, complemented with a seismic module (SCPTu), which allows an optimized parametric deduction with inverse methods (using non-local regularization techniques recently developed, Mánica et al., 2018) and complemented by advanced laboratory tests with undisturbed samples using more suitable sampling techniques (Viana da Fonseca et al., 2019; Molina-Gómez & Viana da Fonseca, 2021).

2.2 Recent case-histories

The sense of loss in human resilience is attained in Brazil recent catastrophes dams's collapse: Fundão, in 2015 (YouTube, 2016, 2018), or Córrego de Feijão mine, B1 dam, Brumadinho, in 2019 (YouTube, 2015, 2019), both in the state of Minas Gerais.

Tailing dams have experienced many flow liquefaction failures, e.g. Stava mine in Italy, 1985, Sullivan Mine in Canada, 1991, Merriespruit Harmony Mine in South Africa, 1994) in Aznalcóllar in Spain, 1997 and Fundão in Brazil, 2015 (Morgenstern et al., 2016). The most problematic dams were constructed using the upstream method with steep inclinations. The liquefaction of the impounded materials suggests that the problem lies with the impounded tailings (Viana da Fonseca, 2013). However, in the absence of internal collapse or induced shear, liquefaction and outflow of ponded ash and tailings occur after the dam has failed. This was not, at the time, considered a complex problem for local designers and consultants, as recognized by Brazilian authorities after several back-analysis reports on the causes. Progressive loss of strength processes can occur along the entire life of the structure. By contrast, most laboratory experiments conducted on tailings samples last from a few hours to weeks. The schematic diagram in Figure 1 enhances some of the numerous factors that condition the knowledge of these materials and the permanent engineering of record that has to stand during the life of TSF.

2.3 Which and when brittle materials (soils) liquefy and cause earth structures to fail

Practice has been revealing that the high number of failures in upstream dams exceeds downstream and centreline tailings dams, and more even in one stage construction, although there are several cases with very high impact where the liquefaction occurred due to brittleness of the foundation soil of the "dike" conducting to liquefaction of the tailings in the reservoir (Gens, 2019). The construction of upstream dams is done during the mining operation, for a predicted volume of storage (and consequently height of the dam/dike), but sometimes additional volumes are considered and new projects approaches are necessary; the re-evaluation of the design conditions (materials properties and system behaviour) is demanding for continuous reassessment, especially when finer tailings or slimes support the additional dykes. Tailings are usually deposited loose, therefore contractive, which means that any actions that induce undrained response can trigger liquefaction (partial or complete) and collapse; around 100 upstream failures in around 3500 tailings dams may be considered a low number but have serious consequences in lives, social resilience due high infrastructural damages and terrible economic and environmental losses.

This is the reason why the present best practice incorporates in the organization of TSF a permanent responsible of Engineering of Record (EoR). At a different level, the Independent Tailings Review Boards (ITRBs) formalized in 2002 by the International Council on Mining and Metals, ICMM (Mishra and Mohanty, 2020), as part of the standards to ensure the best govern practices (Global Industry Standard on Tailings Management: GISTM, 2020), has an important role to provide the owner with an independent opinion of whether the designs, analysis, performance, operation, maintenance, surveillance, and

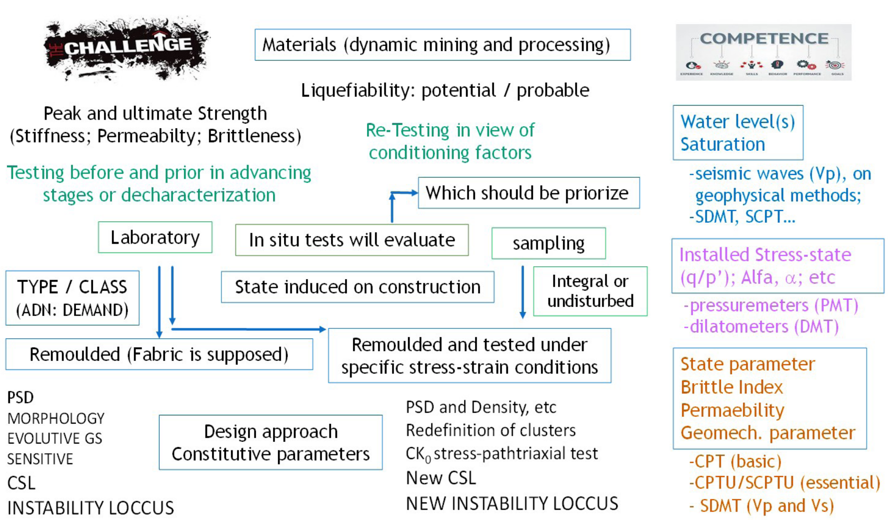

Figure 1. A tentative flow chart of the role of experimental procedures.

assessment of the Dam or Tailings Storage Facility, being consistent with industry standard practice.

Liquefaction is an undrained process that can be static or cyclic, but can also be induced by a drained process, such as an increase of pore pressure incurring in a consistent drop on the mean effective stress with constant deviatoric stress. This is known and from the very early days (Castro, 1969) of Soil Mechanics and in Figure 2 some stress-strain paths in triaxial drained and undrained tests illustrate the hydromechanical behaviours associated to flow liquefaction mechanisms, with correspondence to well documented catastrophic tailings dams' failures (Gens, 2019). As illustrated in Figure 2, adapted from a table in the article of the referred author, (a) overtopping can be due to unanticipated storm runoff , failure of diversion dams and ditches and/or failure of spillways/decants, loss of freeboard, while loss of support is triggered by rapid rate of raising, steepening at crest, and/or construction activities at crest; (b) overloading is a consequence of rapid rate of raising, steepening at crest and and/or construction activities at crest; (c) dynamic/cyclic actions, induced by earthquakes; blasting and/or construction traffic or geotechnical works (like dynamically driven piles, sheet piles or vibrating coring and impact push-in drilling; (d) changes in pore pressure / reduction in mean effective stress, due to drainage malfunction, raising water table; localised leakage; internal erosion and/or inhibited volumetric creep.

Susceptibility for liquefaction means that a specific TSF – with a geometry, materials with intrinsic geomechanical properties and at rest state in terms of density and confined stress – may liquefy under a large variety of dangerous actions, called triggers (Viana da Fonseca et al., 2021a, Reid et al., 2022e). This susceptibility is particularly serious in soils that can present a very high brittleness, observed in the stress-strain on a load-controlled triaxial test in Figure 3, together with the invariant representation of the stress-path, in full or partially (it may happen in the case of existing occlude air bubbles) saturated soils. From that scheme, it can be seen that the ultimate ("residual") strength will be "catch" in very low value ("CS") on Critical State Line (CSL).

For a material to be susceptible to flow liquefaction there are two conditions to be accomplished: (i) the materials should be or at least close to saturation; and (ii) the material should be brittle, to be contractive is a necessary condition

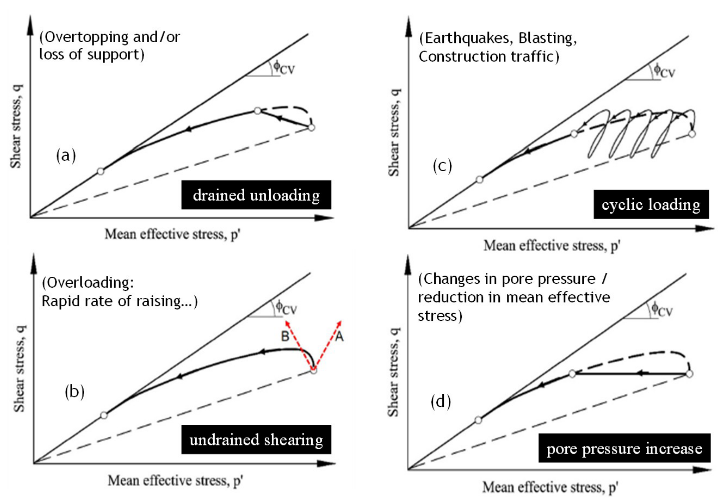

Figure 2. Stress-paths associated with four selected mechanisms triggered in case-histories where partial or full liquefaction instability ocurred (adapted Gens, 2019): (a) Merriespruit (1994), Aznalcollar (1998), Cadia (2018); (b) Fundão (2015); (c) El Cobre (1965), Fundão (2015); (d) Stava (1985) Dam 1, Feijão mine, Brumadinho (2019).

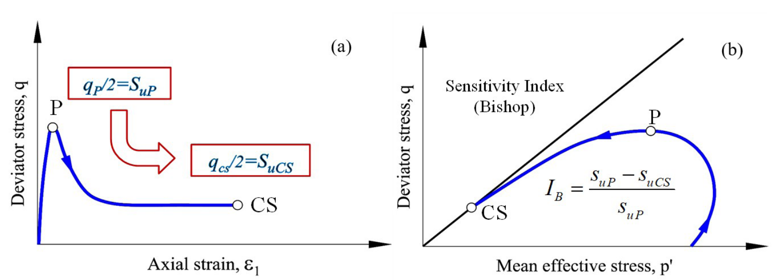

Figure 3. Undrained response in brittle soils (concept of instability and sensitivity).

but not sufficient. In fact, as stressed by Hight & Dias (2023) instability can occur under drained, undrained and partially drained conditions; (iii) under undrained conditions, only very loose sand can become unstable and this can lead to static liquefaction or collapse if the driving shear stress is and remains significantly higher than the ultimate or critical state strength; and, (iv) drained instability in both loose and dense sands only occurs when there is a reduction in the mean effective stress that may result from a decrease in total mean stress (e.g. an excavation) or from an increase in pore pressure (e.g. rising groundwater level).

The mechanism of this "so-called" flow liquefaction or instability is now reasonably well understood, although there are still some uncertainty and controversy regarding some of its specific aspects. Instability is taken to be the behaviour in which large plastic strains are generated before general failure because the soil cannot sustain the applied load or stress. Collapse, yield or static liquefaction are used when the drop from peak (sometimes designated 'yield') to ultimate strength is large and occurs rapidly, usually under load-controlled conditions.

More generally, the condition of a soil undergoing shear strains under constant stress and with no volume change is a key element of the Critical State Soil Mechanics (CSSM) framework and models. An important contribution to the characterization of the behaviour of soils has been the concept of state parameter, which has been incorporated in mainstream soil mechanics (Been & Jefferies, 2011). It is again interesting to note that the development of the state parameter concept was made in the context of providing a rational engineering approach to the construction of structures using non compacted hydraulic sand fills (Viana da Fonseca et al., 2011). Soils become additionally sensitive (fragile) when they have a metastable structural condition. This a consequence of a clustering fabric resulting in non-uniform void distribution and the presence of macro voids, which can exist in the nature or induce by anthropic actions, due to depositional and post-depositional processes (Hight et al., 2023).

The association of flow liquefaction with undrained softening and pore pressure increase was identified in the stress-controlled tests carried out more recently in recognized expert tests, including the geotechnical laboratory in Faculty of Engineering of the University of Porto, FEUP (Viana da Fonseca et al., 2022). The question of the uniqueness of the Critical State Line (CSL) remains under discussion (Narainsamy et al., 2023), although the sense of uniqueness should be unquestionable (Fourie & Tshabalala, 2005; Bedin et al., 2012; Schnaid et al., 2013; Li & Coop, 2019; Delgado et al., 2025). Experimental difficulties to determine its locus are due to the limitation of the axial strains achieved in the triaxial apparatus, the need for area and membrane penetration corrections, accounting for volume changes during backpressure saturation, the effects of strain localization, and incorporating inertial effects in the interpretation of stress control tests (Soares & Viana da Fonseca, 2016). Further research is required at higher strain rates (Viana da Fonseca et al., 2021b; Fourie et al., 2022) and judicious (meticulous) interpretation procedures (Hight, 2024; Delgado et al., 2025).

There are constraints concerning the point of maximum (peak) strength that signal the onset of instability. This is reached with a mobilized friction angle well below the critical state. Because peak strength values increase in an approximately linear manner with mean effective stress, it is tempting to join the different peak state points to establish a kind of failure criteria in terms of effective stresses, which is erroneous. Two different proposals are possible: a collapse line that passes through the steady state point (Ishihara, 1993) and a flow liquefaction line that passes through the origin, reconciling the two concepts based on the state parameter (Yang, 2002).

2.4 Modelling instability

Material instability has been approached from a rigorous theoretical mechanics perspective (Nova, 1994; Andrade, 2009), since in this case, it takes place when the deviator stress reaches the peak strength, being an apparent inconsistency. When an undrained test reaches its peak strength, the material softens and collapses, especially under stress-controlled conditions, while if sheared in drained conditions, there is no visible instability. This paradox is usefully explored using the important concept of controllability. The onset of this novel approach has been implemented recently in a modified CASM model (Clay and Sand Model, (Yu et al., 2005)) by the Polytechnical University of Catalonia, in Barcelona (Ramos et al., 2015; Rios et al., 2016; Monforte et al., 2019; Mánica et al., 2022). This geomechanical modelling innovation, as described by Gens (2019), is simple, state dependent (it can mimic classical critical state models by selecting appropriate parameters), non-associated and incorporating instability phenomena. It will be called from here onwards "CASM-Liq".

This discrepancy in time scales demands for continuous monitoring of the stability of these structures in time, by conducting analyses with reliable advanced constitutive models available in accessible numerical tools (like Plaxis®), capable of effective stress-strain analyses with hydraulic coupling on soils exhibiting undrained softening. Advanced numerical procedures currently exist, enabling large deformations analyses, through the various formulations including the Particle Finite Element Method (PFEM), already tested in selected results of cone penetration tests in an undrained softening material (Gens, 2019). Given the importance and frequent catastrophic consequences, a large amount of research has been performed on flow liquefaction More generally, the condition of a soil undergoing shear strains under constant stress and with no volume change is a key element of the Critical State Soil Mechanics (CSSM) frameworks and models.

3. The case Dam 1 in Brumadinho – a benchmark case-history

3.1 Description of the dam structure and the official analyses of the rupture

Quoting the description in Viana da Fonseca et al. (2022), Dam 1, approximately 85 m high, in the municipality of Brumadinho, suddenly failed at 12:28 p.m. local time on January 25th of 2019, after more than forty years of operation and deposition of tailings processed from the natural rocks extracted from the Córrego de Feijão mine of the Paraopeba Complex, in Minas Gerais (MG), Brazil. The recorded images showed that the dam failure was sudden and abrupt, with no apparent signs of distress prior to the failure, developing across approximately 80% of the face of the dam in about five seconds. The failed slope material quickly turned into mudflow (Figure 4).

The tailings with a very high percentage of iron, with very heavy solid particles, had no plasticity and their grains were mostly silt-sized, deposited from a water suspension and were generally very loose (void ratios around one). The tailings were not homogenous, having finer and coarser gradings with no bonding. Finer gradings had lower permeabilities and more contractive structures - as indicated by state parameter values. Although the critical state friction angle, was similar for all gradings, finer gradings also had a lower capacity for mobilizing strength in undrained conditions. That happened also at peak, but it is more noticeable at the critical state. Consequently, finer gradings were more prone to liquefaction and more dangerous, because more brittle. A good part of these conditions was identified with thorough most mortem analyses of integer recoiled samples as well as some undisturbed samples tested in well-equipped geotechnical labs. Additional data was collected from the reinterpretation of a large number of in situ tests executed before the accident, particularly the ones more recent, which included very good CPTU and SDMT. In this work, the author describes some of the options conducted in tests and the interpretation of their results, in order to define the hydro-mechanical properties of these non-textbook soils to evaluate the stability analyses that could help to determine the causes of that failure.

Two very detailed works have been contracted by Vale to explain what may have occurred:

- the Expert Panel Technical Report (EPR) by Robertson et al. (2019);
- the CIMNE/UPC Computational Analysis Report of by Arroyo & Gens (2021).

For this last study, the Geotechnical Laboratory (LabGEO) of the Civil Engineering Department at the Faculty of Engineering of the University of Porto (Portugal) was invited to conduct the advanced testing program, using appropriate methodologies that could provide the parameters for the constitutive models in numerical simulations. The laboratory procedures included the reconstitution of representative specimens in diverse state conditions and the execution of a wide variety of both conventional and advanced laboratory tests in these specimens. Undisturbed samples were recoiled in the vicinity of these integral samples, which allowed for extra information explored for some analyses of the influence of structure in these conditions (fabric and/or cementation) in the options of the calibration of models for stress-strain numerical analyses in CIMNE report (Arroyo & Gens, 2021). Details of this sampling campaign and FEUP lab tests are in the Annex A of that report.

3.2 Appropriate lab systems and experimental procedures in reconstituted samples

In this study, a series of advanced triaxial tests were carried out using triaxial cells with lubricated end platens

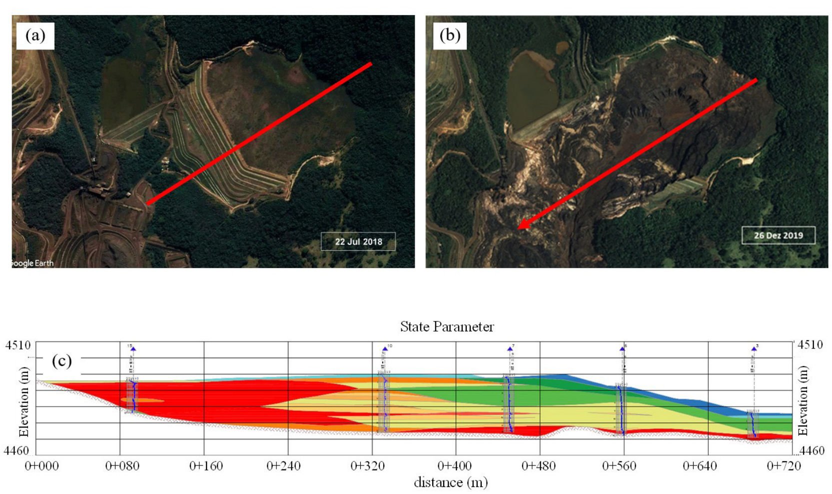

Figure 4. Google Earth images of dam 1: (a) in 2018; (b) after collapse (adapted from Viana da Fonseca et al., 2022); (c) identification of materials clusters (adapted from Arroyo & Gens, 2021).

(LEP) and an embedded connection piston (ECP), into the top-cap, and a Bishop-Wesley type stress-path triaxial cell equipped piezoelectric ceramic instruments (Figure 5). Bishop-Wesley triaxial cell used in this study can apply numerous combinations of stress-path using an automatic control system.

The piezoelectric ceramic instruments (bender elements, BE, transducers) allow measuring the seismic wave velocities in the soil sample through specific interpretation methodologies (Viana da Fonseca et al., 2009). All specimens were prepared from the remoulded material, after homogenization (Viana da Fonseca et al., 2022) and using the undercompaction moist tamping method (Ladd, 1978) for different aimed void ratios and tested in fully saturated conditions. The saturation process was carried out according to the procedures recommended by Viana da Fonseca et al. (2021) to assess the critical state locus (CSL) of cohesionless soils. The full saturation was confirmed by Skempton's B-value > 0.97. The critical state locus was estimated from several isotropic (K = 1) drained and undrained triaxial tests on loose specimens, which reached the ultimate state. Besides, a series of loose specimens were anisotropically consolidated ($K\neq1$) and then subjected to triaxial shearing to more accurately reproduce the in situ conditions occurring in the TSF. Notwithstanding, dense specimens with distinct state parameters were tested to derive a stress dilatancy relationship, as suggested by Jefferies & Been (2016). Finally, a series of drained and undrained extension tests were carried out on loose and dense anisotropically consolidated specimens to evaluate the tailing strength parameters in extension conditions. These tests were conducted under anisotropic consolidation and sheared by decreasing the axial stress, ensuring the inversion of principal stresses.

For the triaxial cells with LEP and ECP the end-of-test soil freezing (EOTSF) technique was implemented, whereas for the Bishop-Wesley type stress-path apparatus, the specimens were carefully removed from the cell, avoiding possible loss of soil particles and water (Verdugo and Ishihara, 1996). The EOTSF was not used during the tests conducted in the Bishop-Wesley type stress-path to avoid damage to the piezoelectric ceramic instruments. Both procedures provide similar results when applied properly, as suggested by Murthy et al. (2007). A series of oedometer tests were conducted on remoulded specimens with different initial void ratios (e_0) to examine the potential transitional behaviour of B1 iron ore tailings. This was included in a first phase studied by CIMNE/UPC and FEUP taking the three class of samples that could be taken as representative of the materials involved in the collapsed masses on the 2029 and summarized by Viana da Fonseca et al. (2022). Later a fourth sampling campaign was possible due to extra safety conditions in the failure zone, which is described in Viana da Fonseca et al. (2023) and Delgado et al. (2025).

3.3 Four representative types of soils considered for zonation of the mass

3.3.1 Particles' physical characteristics

The considerations that will be done hereby will be focused in the studies on the iron ore silty and sandy tailings from Córrego do Feijão mine in Brumadinho (Brazil). The campaigns to collect representative samples of these tailings were carried out in two phases, comprising four sites in the remains of the Dam 1. In the first phase, in December 2019, three of these collections were done (type 1, 2 and 3), with some limitations to access to the bottom of the rupture zone. As described in the annex of report of CIMNE/UPC, this classification of three clusters of distinct classes of soils, allowed to identify three corresponding sets of constitutive parameters to be assumed for the extensive numerical studies that were developed in what followed (Arroyo & Gens, 2021). The collected integral samples were considered representative

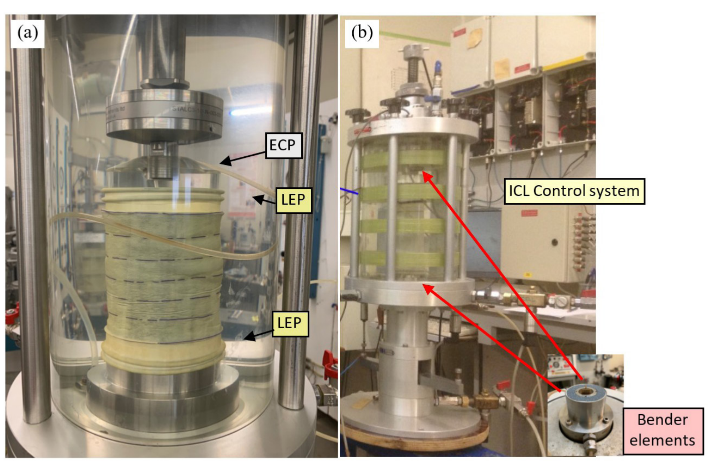

Figure 5. Advanced triaxial equipment: (a) Conventional Tx cell adapted with LEP and ECP; (b) Bishop-Wesley type stress-path with Imperial College of London control system.

materials of the soils composing this TSF. The analyses of the materials collected at that time have different physical, hydraulic and mechanical properties that were resumed in Viana da Fonseca et al. (2022), colour and distinguishing iron and fines contents that were identified with a quantitative procedure based on the analysis and comparison of particle size distribution and specific gravity of solid particles results (Figure 6). Soil type 1 corresponds to fine reddish, low-ferrous tailings, with a specific gravity of 3.94. Soil type 2 refers to a fine brownish, moderately ferrous tailings, which specific gravity is equal to 4.55. Soil type 3 is a coarse-grained black iron-rich tailing, with the highest specific gravity of 5.00.

The last soil (Type 4) was collected in a second phase (latter March 2020), when the access to the deeper layers was safer. In Figure 6a the three types are outlined while the range (a fuse) of results obtained in previous campaigns is drawn. In Figure 6b the type 4 material is also plotted. The distinct particle densities are related to the initial stages of tailings deposition, when processes of extracting iron ore from the rocks was less efficient. The percentage of iron is higher in the blackish tailings, produced in the first rising phases of the dam (reference samples of type 3 and 4 had up to 96% and 95% of Fe_2O_3), in comparison to the brownish (Type 2) and reddish (Type 1) tailings, corresponding to more recent operations with lower iron content (respectively, 84% and 67%).

The projected position of type 4 soil in the tailings pond, identify as S3-L1 in Figure 7, and its relation to the first phase sampled three types of soils (S1 included "Type 1"

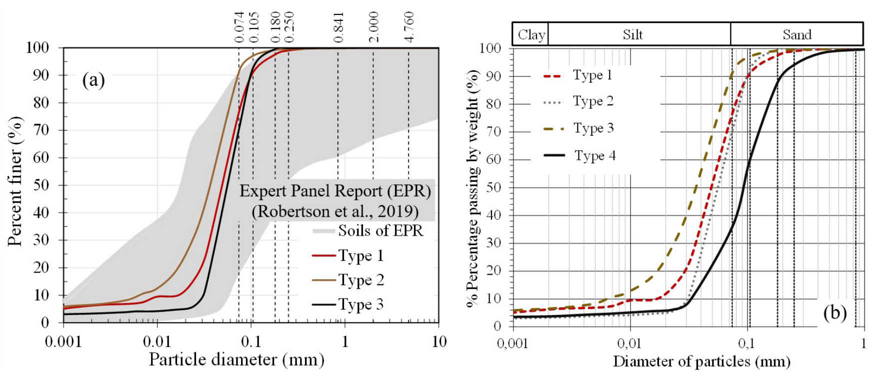

Figure 6. Grading curves of Córrego de Feijão tailings: (a) three types of two initial campaigns and other soils (adapted from Viana da Fonseca et al., 2022); (b) soil Type 4 comparison with other tailings.

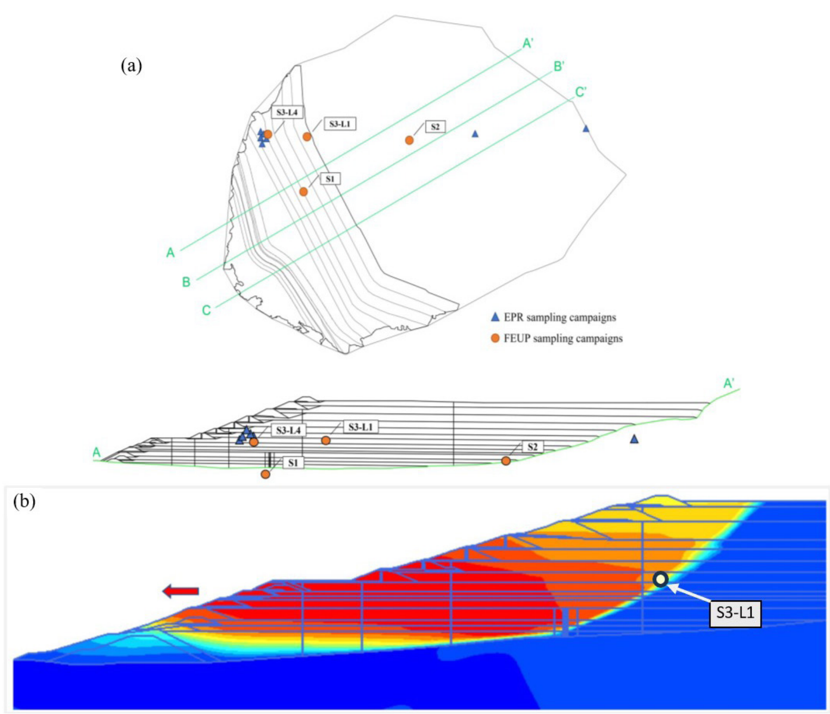

Figure 7. Location of sampling collection in the S3-L1: (a) Projected position in the plan view of the dam and alongside the dam section (Viana da Fonseca et al., 2022); (b) Failure zone (Arroyo & Gens, 2021).

and “Type 3” and S2, another, Type 2”), is exhibiting that this site is below the third rising at the left abutment of the dam, where the failure surface initiated and propagated. In this site, a significant amount of integral remoulded samples of iron, and some undisturbed blocks of were collected at that depth.

3.3.2 Intrinsic properties: oedometric and isotropic compressibility and hydraulic conductivity

In Viana da Fonseca et al. (2022) the main conclusions from the oedometric consolidation tests performed to assess the compressibility of the three types of tailings of the first phase are presented. Based on these oedometer test results it was observed that the three types of tailings exhibited a slope change on the compressibility curve for effective vertical stresses (σ'_v) above 3200 kPa. This finding evidences the evolutive nature of these soils, caused mainly by particle breakage (or crushing) or by changes in particle shape (morphology) at higher stresses. On the other hand, no transitional behaviour was observed in these materials, since tests performed at different initial void ratios converged to the same 1D compressibility line.

Isotropic consolidation tests carried out in triaxial cells were also performed on remoulded loose specimens applying several consolidation stages, with measurement of the volumetric change over time, permeability could be estimated by the time of consolidation, in order to have a more reliable determination of the hydraulic conductivity and its confinement stress dependence. Since the triaxial cells used for these tests were equipped with bender elements (BE), seismic shear wave velocities, *Vs*, were measured to estimate the variation of the small-strain stiffness at each consolidation stage, according to the methodology proposed by Viana da Fonseca et al. (2009) and Ferreira et al. (2021). This aimed to study the influence of the interparticle rigidity in the gomechanical behaviour. In addition, seismic compressional wave velocities, *Vp*, were measured to assess saturation conditions, complementing the verification by Skempton’s *B* parameter, as recommended by Viana da Fonseca et al. (2021).

The hydraulic conductivity or permeability of particulate materials is a function of the particle size distribution, their morphology, therefore the specific surface. In fact, the best models include at least these parameters to account for the relationships between the flow rate and the porous space, such as the size of the pores, their tortuosity, and their connectivity (Chapuis & Aubertin, 2003). These authors give an overview from the original relationship proposed by Kozeny in 1927 and later modified by Carman in 1937 (KC method) and updated in 1956 (KC method). The classical KC equation is approximately valid for sands and is not valid for clays, and mostly because of the difficulty to determining the soil specific surface (*S*). Chapuis & Légaré (1992) proposed a method for estimating the specific surface of a nonplastic soil from its complete grain size curve. In the cited work from 2003, the authors have tested the applicability of the KC with the Chapuis & Légaré (1992) method for estimating the specific surface to predicted k values in mine tailings, concluding that they do not match with measured k values in the case of mining tailings. The reason for that is that the fine particles of tailings are angular, sometimes acicular, which introduces an increased effect of tortuosity, implying in void space very different from the void space of a natural soil. Recently new approaches tendo to create new formulations of permeability assessment in mine tailings, which present systematically lower permeabilities of natural granular materials, sandy with distinct silts’ contents, with similar PSD. This was clearly identified in the work of Fan et al. (2022), who identified there was a more than 20-fold decrease in hydraulic conductivity, k, for increasing fines content from 12% to 50%; while the impact of fines on k was negligible for fines contents greater than 50%. k for the tested specimens with varying fines content from 12% to 100% was proportional to $[e^3/(1+e)]$ and inversely proportional to S^2, where *A* is a factor describing the effect of angularity in particle shape and *S* is the specific surface for the fines and sand grain mixture (*S* increased linearly with increasing fines content). In addition, tailings are prone, namely, to the creation of new fines during compaction. Chapuis & Aubertin (2003) worked with several mine tailings, predominantly silty, and proposed the best-fit equation for the examined materials:

$$\log\left[\frac{k}{1m/s}\right] = 1.5\left\{0.5 + \log\left[\frac{e^3}{D_R^2 \cdot S^2 \cdot (1+e)}\right]\right\} + 2 \quad (1)$$

k value of intact saturated samples of tailings cannot be predicted by the KC equation because intact tailings are typically finely stratified (cm or mm scale) and have a high anisotropy in *k*. The equation of Fan et al. (2022):

$$\log k = \log\left(\frac{Cg}{\upsilon_f \cdot \rho_s^2}\right) - 2\log(S) + A \cdot \log\left(\frac{e^3}{1+e}\right) \quad (2)$$

where *A* is a factor describing the effect of angularity in particle shape.

Tailings from B1 in Brumadinho present average (in 20 determinations) of morphological indices ranging, respectively in T1-Type1, and T3 -Type3, of the high aspect ratios (0.78, 0,79), very low roundness (0.38, 0,40), moderate elongation (0.55, 0.48) very high convexity (0,94, 0.93) and straightness (0,99, 0.99), In this facie it is expected that permeability being dependent on the particles’ angularity and specific surface area which tend to increase with fines content. As a matter of fact, Chapuis & Aubertin (2003) studied the applicability of KC equation for mine tailings proposing a slight modification to the equation including a parameter *A*=1.5. Data results of copper tailings presented by Fan et al. (2022) have pointed out *K* of 2 to 2.5, while in B1 iron ore tailings this constant can double the reference of 1.5

for natural sands. This line of research must be developed, as this will have high implications in the drainage capacity of TSF under more or less rapid loadings.

Still, the three types of tailings measured by direct constant head permeability tests measured in triaxial cells, under distinct confinement effective stresses, were decisive to have reference values for the analyses of the drainage grades that would be needed for the zonation of the tailings pond in view of the complex coupled stress-strain numerical analyses. The variation of k for the three tailings as a function of the effective stresses and void ratio conditions have quite distinct trends which is a clear indication of distinct soil behaviour, although de PSD is not so different (Viana da Fonseca et al., 2022).

In Type 4 soil, from the second phase of sampling, the intrinsic properties (colour, specific unite weight – density) of the particles and morphology mostly converged with the related soil (Type 3), both being blackish, with heavy particles densities and morphology, therefore similar compressibility and hydraulic conductivity trends (Viana da Fonseca et al., 2023).

3.4 Critical state lines: are they intrinsic mechanical properties?

3.4.1 Deviatoric stress and volume vs mean effective stress isotropically consolidated and vertical compression

An evolution of the mechanical behaviour of the studied tailings was observed in the first phase three type of tailings. The evolution of the soil behaviour caused additional compressibility –represented by a shift down of CSL in the *e*-log *p´* plane. However, it did not affect significantly the friction angle of shearing resistance at the critical state (Figure 8a). Such an evolution was attributed to some increase (slight) in fines, but essentially to changes in the morphology of soil particles (Figure 8b). Figure 9 presents SEM images of two soils (Type 4 and 1) in as sampled in situ and evolved after high pressures, illustrating the change in morphology (higher in the lower sized tailing).

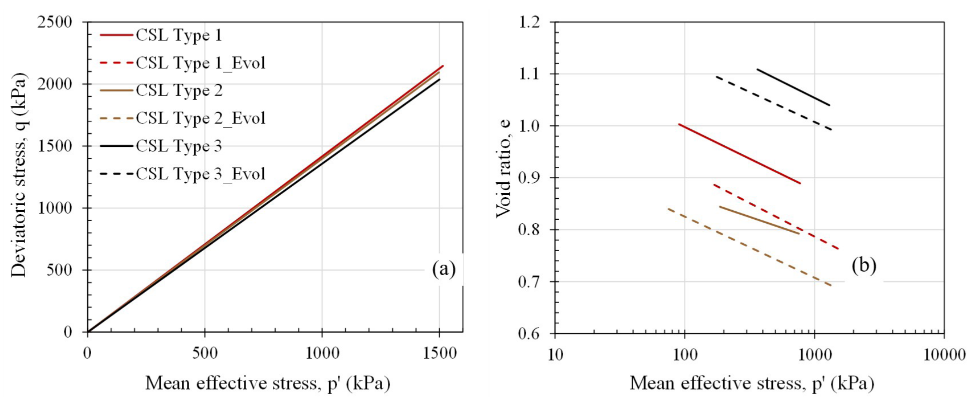

Figure 8. CSL of the three tailings in natural and evolved conditions in the: (a) q - p' plot; (b) e – log p' plane (Viana da Fonseca et al., 2022).

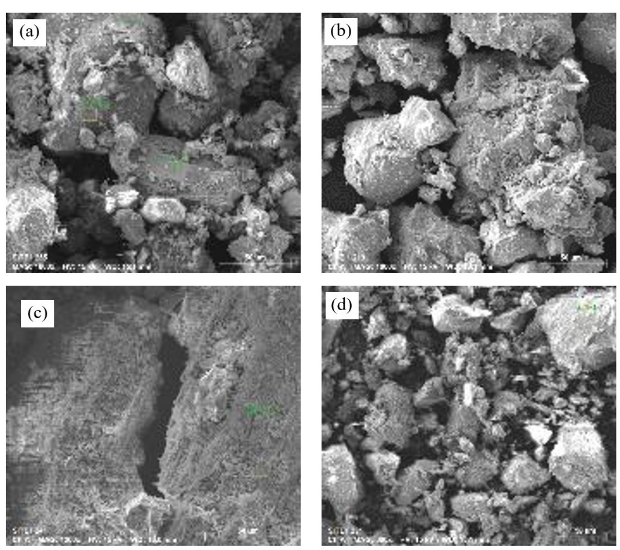

Figure 9. SEM images of Type 4 soil (black with coarser PSD and higher % of iron): (a) natural; (b) evolved; and Type 1 (reddish soil with finer PSD and lower % of iron): (c) natural; (d) evolved.

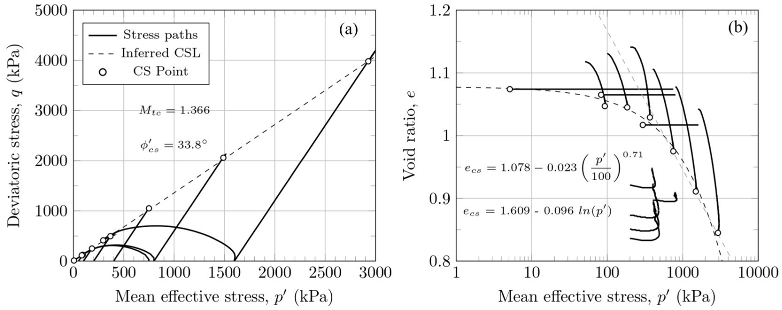

Figure 10. Inferred CSL of tailing Type 4 (after Viana da Fonseca et al., 2023): (a) p'–q invariant space; (b) e – ln p' invariant space.

The average values of the shape factor are not very distinct in between the four types in terms of Aspect Ratio (≅0,78); Convexity (≅0,93); Elongation ((≅ 0,50) Sphericity (≅ 0,83); or Straightness (≅0,99), while on Roundness there is a difference between the blackish with higher % of iron and particles density (Type 3/4 ≅ 0,38), while the reddish, with lower % of iron and particles density (Type 1 ≅ 0,46), which may denote a slightly higher sensitivity of these ones. Still some investment must be done on determining the roughness of the particles as this can be a decisive factor for distinct behaviour. This distinction from smooth and rough particle demands for fractal analysis of particle contour is promising, which is now promising (Hyslip & Vallejo, 1997; Guida el al., 2017).

The determination of the critical state line in Type 4 tailings was determined with the same referred procedures, but at this time with more extensive and diversified conditions. The results of all drained and undrained loose triaxial tests have reached the critical state being used to define the critical state parameters (in Figure 10).

The stress-dilatancy relationships of the soil in this study were obtained from a set of drained triaxial tests on dilative samples with distinct state parameters (interpretation in Viana da Fonseca et al., 2023). It has observed that these have not been adopted to define the CSL e–p' since dense specimens are susceptible to localisation therefore critical state condition is attained only locally, “circumscribed” nut not overall shear bands (Desrues et al., 1996; Jefferies & Been, 2016; Salvatore et al., 2017).

Due to the high instability of the tailing Type 4, the CSL in the e–ln p' invariant space can be approximated using a power law relationship as follows:

$$e = A - B \cdot \left(\frac{p'}{p_{ref}} \right)^{C} \tag{3}$$

where A, B and C represent three material constants while p' and p_{ref} are the mean effective stress and reference stress condition, respectively. The CSL projection in the q–p' space define a strength parameter M_{tc} equal to 1.366 and angle of shearing resistance of ϕ'_{cs} of 33.8º.

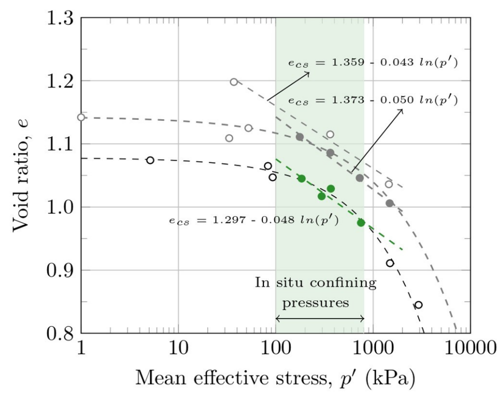

Figure 11. Comparisons between CSL (after Viana da Fonseca et al., 2023).

Physical properties of this soil (Type 4, similar to Type 3), are similar to Type 1 and 2 soils, with low particles density differed in colour, iron content and hydraulic conductivity. In Type 4 tailing, the compressibility and CSL have higher sensitivity to the variation of the state, that is, a stronger non-linearity stress-states and stress-paths (in compression and extension shearing). This is well seen in Figure 11, with emphasis to the clear nonlinearity of CSL.

In the first parametric evaluation based on few tests on type 3 soils (Viana da Fonseca et al., 2022) that line was assumed linear, as a simplification for the calibration of the parameters in CASM model used for the numerical simulation (Besenzon, 2024). That hypothesis was considered in view of the stresses that were involved in the main volume affected by the failure mechanism of Dam 1. These were limited in a range of around 100kPa and 1MPa (shaded area in Figure 11), where the quasi-linear CSL may be acceptable at those stress levels. Future analyses should consider this non-linearity for any other extra analyses involving different stress levels.

3.4.2 Critical State Lines for distinct inherent and induced particle structure

There has been an extensive discussion on the influence of factors that can indicate the non-uniqueness of the

CSL. Studies conducted twenty years ago, like in Finno & Rechenmacher (2003) and Fourie & Tshabalala (2011), and more recently by Rabbi et al. (2018) or Silva et al. (2024) have provided evidence that the CSL is influenced by the consolidation history of soils. In the last two cited works in iron ore tailings from the "quadrilateral" of Minas Gerais, Brazil, a slightly lower critical state stress ratio (M) can be observed in triaxial tests in compression towards in extension tests, particularly if consolidated in K_0 conditions lower that 1, due to the more severe long stress paths – especially imposing an increase of the mean effective stress (lateral/radial confinement), which in undrained load conditions generate higher increase of pore pressures. Chu & Wanatowski (2008) demonstrated that while the CSL remained unchanged for different types of consolidation, its elevation was found to be dependent on the inclination of the principal stress angle to the vertical and horizontal directions (α) or the Lode angle. The difference in the Lode angle ($\theta = \pi/6$ for triaxial compression; and $\theta = -\pi/6$ for triaxial compression) can explain this small "distinct" inclination, buy the fact that in extension the intermediate principal stress is equal to the major principal stress. However, the variation of M does not imply in the critical state friction angle. In what respects to the critical state line (CSL) in the specific volume e-log p' plane, the points for the range of the studied stresses, with the specimens moulded at different but loose void ratios (positive state parameters converged towards a unique curved CSL, which is mostly concurrent works Bedin et al. (2012) and by Li et al. (2018) for gold tailings, by Carrera et al. (2011) for fine sand and silt and, partially, and by Li & Coop (2019) for iron ore tailings.

Paradoxically, in another work from Wagner et al. (2023) in two samples of iron ore tailings, although confirming a similarity of the critical state friction angle, slightly higher for extension tests, the CSL on plane on e-log p' are both curved, but the conclusion is opposite of the previous works, that is authors suggest that in spite of lower strain being reached, suggested that the location of CSL for extension tests does not converge to the CSL defined for compression tests. This should not be assumed, and this can in fact be due the fact that the triaxial extension were limited to too low strain levels, probably due to premature localization (necking) in extension loading. This is particularly the case for moist tamped specimens that can develop easily non-uniformity in the case of extension. Stopping the tests at low axial strains and calling that "critical" is not acceptable interpretation. Being the extension tests consolidated to states far from the extension CSL they are likely to exhibit phase transformation. This could not be taken as points of the CSL, the same erroneous assumption in the work from Fotovvat & Sadrekarimi (2022), who have also defended the non-uniqueness in the e-ln p' plane due to deformation mode and strain direction. Recent works (Becker et al., 2023; Salvatore et al., 2017) proved that it is mostly probable that CSL in compression and extension is the same, if effort is made to consider localisation behaviour of the samples in extension, namely examining the localisation issues recurring to using photographic correction. Other information referring to this important clarification of how to define CSL are discussed in Li & Dafalias (2012).

In a recently published article (Corrêa de Oliveira et al., 2024) the critical state lines (CSL) of two extensively studied iron ore tailings with different fines content were investigated which proved to be clearly curved in the e-log p' plane, with a flat trend at low mean effective stress, indicating the instability of these materials in looser conditions. As the confining stress increased, there was a reduction in strain-softening response, and CSL became steeper and parallel to the respective consolidation line. For the tested confining pressures, although marginal, indications of grain breakage were observed, especially for the coarser tailings. This suggests that the steeper slope of CSL at higher mean effective stresses is associated with the particles' morphological evolution (shape and surface roughness) and particle breakage. The K_0-consolidated tests showed minor significance in the CSL definition, unlike the instability line, which is strongly influenced by induced anisotropy, with a tendency to increase 'η_{pk}' (or 'η_{IL}') and approach the CSL. It should be noted that the variation of the CSL slope in q–p' plane with θ can be estimated by typical mathematical relationships available in the literature (Van Eekelen, 1980; Jefferies & Shuttle, 2011). Nevertheless, the adoption of a unique CSL regardless of the initial state conditions should not be automatically assumed without further investigation, especially in liquefaction studies. In this case, instability locus may complicate some assumptions, and this has been intensely debated recently, on discussing the implication on Undrained Strength Ratio (3.5.4).

3.5 Instability locus: peak undrained behaviour and residual strength

3.5.1 What is instability and how can it be defined

Instability occurs when soil behaviour rapidly develops large plastic strains, generating afterwards a sudden general failure while soil cannot sustain the applied loading system; that failure, sometimes associated to collapse or static/flow liquefaction, drops the stress state from a peak value of deviatoric stress to ultimate strength rapidly, usually under load-controlled conditions. This occurs inside the failure surface and so is not synonymous with failure, although leading to catastrophic events (Lade, 1993). Contrary to the CSL, inter and intra-particulate structure, has a high influence on the soil behaviour. Fabric in reconstituted specimens by slurry deposition, moist tamping and dry pluviation techniques do not necessarily generate the best matching with hydraulically placed tailings, by one side, and dry stack compacted piles, by the other. The shape and anisotropy of the collapse surface may not be correctly represented, if the preparation method is not well adjusted to the expected filed conditions (hydraulic or compacted and in this case, when done in the wet side or dry side in relation to the optimum compaction moisture content. This is even more accentuated in TSF deconstruction, when different stress paths are applied (lateral extrusion, essentially the horizontal stresses decrease while the vertical stress is kept constant). Drained instability in both loose and dense sands only occurs when there is a reduction in the mean effective stress that may result from a decrease in total mean stress (e.g. an excavation or and extrusion, the probable cause of Fundão Dam, Morgenstern et al. (2016)) or from an increase in pore pressure (e.g. rising groundwater level, one of the hypothesis for the causes of failures identified by Robertson et al., 2019).

3.5.2 The inherent and induced anisotropy in undrained behaviour

The instability locus has been recognized to be dependent on fabric constructed during in field deposition process and the one that is created on the specimens reconstituted using moist tamping sample preparation methods or others. This can be partially solved, in the case of hydraulic deposition, if moist tamping is used with very light spooning, while in the case of reproducing the compaction processes used in dry stacks and piles by using gyratory compactors combining a high precision load mechanism with rigid frame assuring maximum accuracy. This equipment that should be available in the laboratories responsible for the characterization of tailings, particularly the definition of critical states and instability locus, are now well described in recent publications (Viana da Fonseca et al., 2021b; Reid et al., 2021, 2022a, b, c, d, 2023; Fanni et al., 2022, 2024, 2025). The area requiring additional focus in the context of the discussion of the relative direction of the principal stresses in relation to the vertical and horizontal directions (α) effects, is the in situ value of K_0. For instance, the use of parameters defined from triaxial tests conducted in distinct consolidation ratios ($K = \sigma'_v / \sigma'_r$) is now being assessed and the calibrations of the models should be settled for more realistic ratios. NorSand with the Cadia parameters, for instance, produced relatively high K_0 values (Jefferies et al., 2019), leading to significant principal stress rotation. As such, further parametric assessments under a wider range of K_0 values than can be produced with the NorSand model should be carried out.

In the numerical studies described by CIMNE panel (Arroyo & Gens, 2021), the phases conducted to establish the initial conditions (stresses and pore pressures) of the analysis considered the layout of the natural foundation. Pore pressures are obtained from a steady state hydraulic calculation using the boundary conditions specified. Displacements generated during these first phases are reset to zero so that they do not interfere with the displacements computed during construction. At the end of the construction phasing the at rest states were quite diverse in distinct zones of the TSF, from the dam crest to the deposit interior with values close to 0.5.

Some representative stress-strain paths of the test performed to assess the undrained behaviour are presented in Figure 12. This equipment complies a Bishop-Wesley type stress-path triaxial cell equipped with piezoelectric ceramic instruments during any phase of the control, under distinct consolidation ratios and shearing under universal stress-strain paths. The stress-induced anisotropy consolidation was done by increasing both axial and radial stresses following a constant relation $K = \sigma'_v / \sigma'_r$, under distinct values.

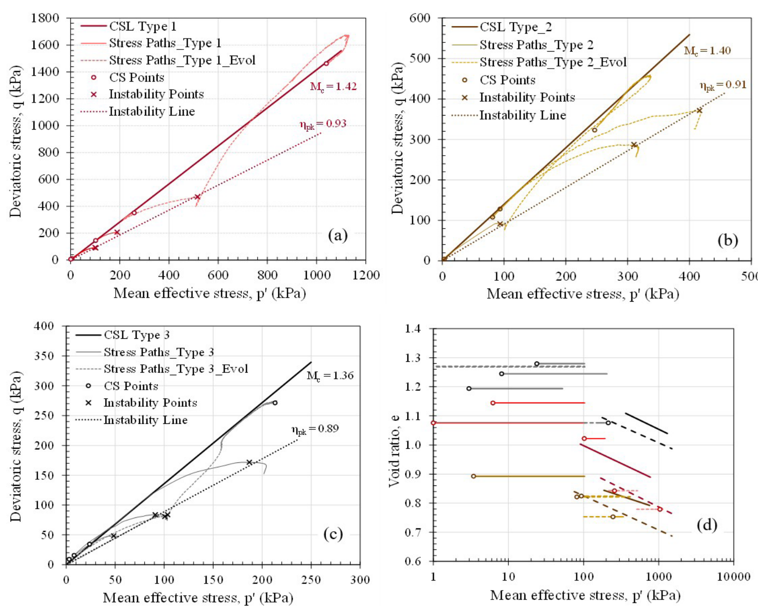

Figure 12. Undrained paths on the q - p' and e - log p' plane for the different types of tailings.

At a research level hollow cylinder apparatus should be explored increasingly to evaluate the effect of anisotropy on instability in undrained loading conditions. In order to address these aspects, laboratory testing was carried out on sandy silts and silty sands tailings in recent extensive studies (Reid et al., 2022a, b, c, d; Fanni et al., 2022, 2024, 2025).

Generally, only very loose sand can become unstable leading to static liquefaction or collapse, or if the driving shear stress remains significantly higher than the ultimate or critical state strength. Specific stress paths which cross the collapse surface, including those involving increasing pore pressure or rotation of principal stress directions, both at constant deviator stress, can cause runaway failure under load-maintained conditions or strain softening under strain-controlled. Drained instability in both loose and dense sands occurs when there is a reduction in the mean effective stress that may result from a decrease in total mean stress (e.g. an excavation or extrusion) or from an increase in pore pressure (e.g. rising groundwater level). In this program of tests all loose samples exhibit positive pore water pressure, revealing the tendency to contractive response over a wide range of confining pressures, as for the dense samples, a stable behaviour was observed. Some of the loose samples presented full liquefaction, with the annulment of the mean effective stress and deviator stress, while others suffered severe strain softening but with not full liquefaction (i.e., zero effective stress), as a stable critical state is reached. In practice, both instability mechanisms would lead to catastrophic results. The undrained tests featured on 2 highlighted the undrained brittleness in the tailings.

The peak strength points for those samples that experienced instability mechanisms allowed the definition of the instability line (*IL*) in the q - p' plane. The stress ratio ($\eta_{pk}=q_{pk}/p'_{pk}$) $\eta_{pk}=q_{pk}/p'_{pk}$)at which the peak is reached is about 0.93, 0.94 and 0.89 for the tailing type 1, 2 and 3, respectively. The uniqueness of the instability line in the stress invariant plane is assumed for each soil, but, while these criteria have proven useful for limit equilibrium calculations, it is difficult to implement as calibration constraints in the context of numerical modelling (Mánica et al., 2022). From an implementation standpoint, the normalized undrained strength ratio ($s_{pk}=s_{u,pk}/p'_0$($s_{pk}=s_{u,pk}/p'_0$) is preferred. It offers a good template description of undrained peak strength in materials exhibiting static liquefaction and is the ratio between the peak undrained strength ($s_{u,pk}=q_{pk}/2$ $s_{u,pk}=q_{pk}/2$) and the consolidation mean effective stress (p'_0). Figure 13 shows the relationships between the undrained peak strength and the consolidation mean effective stress derived from the undrained triaxial compression tests that exhibit instability mechanisms.

3.5.3 Factors that condition peak and residual strength

The undrained isotropically consolidated tests presented in the CSL section were also added for comparison. The interesting aspect is that while the peak undrained strength normalized by the consolidation mean effective stress (p'_0) varies, although the inclinations of the instability line is unique, η_{IL} (Figure 13). The normalised undrained strength ratio with the consolidated vertical effective stress, corresponding to a hypothetical at rest condition, defined as (S_{un}):

$$S_{un} = \frac{S_{u,pk}}{\sigma'_{v0}} \tag{4}$$

Is also very different in clearly different consolidation ratios ($K = \sigma'_v / \sigma'_r$) depending on the type and condition of the soil on the consolidation path, presenting much larger values of S_p for anisotropic consolidation than for isotropic. The underlying reason is that soil fabric is strain-path dependent (Fourie & Tshabalala, 2011). S_p or S_{un} are dependent on fabric associated with anisotropy associated to particles orientation, which is of particular interest to be taken into consideration when modelling the behaviour of these soils.

In Figure 14, the uniqueness of the instability line in the stress space is well defined, as the undrained peak

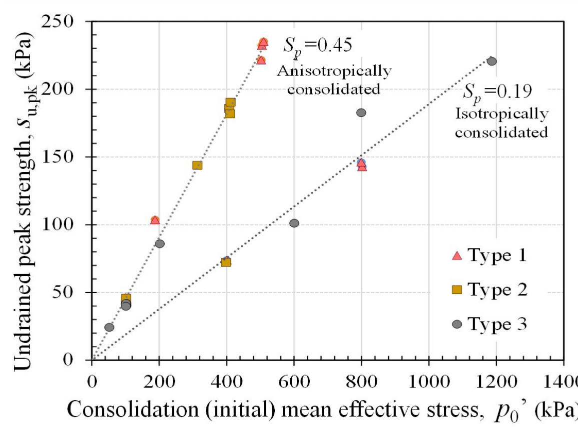

Figure 13. Relation between peak undrained strength and pre-shear consolidation pressure.

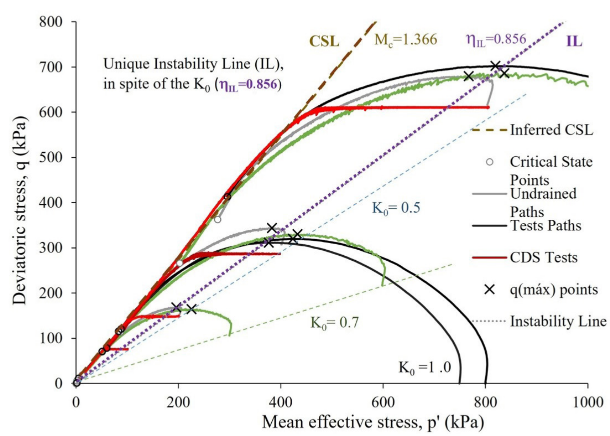

Figure 14. Undrained paths in $q – p'$ and $e – \ln p'$ invariant space.

strength for both isotropic and anisotropic (K=0.5 and K=0.7) consolidated tests align on the same linear locus. Such linear criteria have proven useful for limit equilibrium calculations, but they are difficult to implement as calibration constraints in the context of numerical modelling.

It's quite interesting to look at the results with stress-path control, increasing pore-pressure at a constant rate ("*CDS* tests"), while keeping the deviatoric stress (steady rising of water level by flowing water into the specimen – from the bottom of the cell). The *CDS* stress paths goes towards the CSL, merging with stress-paths of undrained compression tests, closer to CSL.

Figure 15a shows the relationships between the undrained peak strength and the consolidation's vertical and mean effective stresses derived from the loose undrained triaxial compression tests mentioned in this work. The interesting aspect is that the normalized undrained strength ratio depends on the consolidation path, presenting much larger values of S_p for anisotropic consolidation than for isotropic. The level of anisotropy was also reflected with increasing values of S_p with decreasing K. The strong influence of the consolidation path on the peak undrained strength of this tailing was not a surprise. As already referred, Fourie and Tshabalala (2005) observed the same behaviour on the Merriespruit Dam tailings, for instance, and attributed it to the different fabrics that were created during the different consolidation paths. The undrained tests featured in Figure 15b also highlighted the undrained brittleness in the tailings. The axial strain required to reach peak strength was extremely small ($\varepsilon_{a\ pk} \approx 0.90\%$ for isotropic tests and $\varepsilon_{a\ pk} \approx 0.06\%$ for anisotropic test), leading to a rapid strength loss under undrained conditions (i.e., brittle response).

The type of material and inherent anisotropy due to distinct ratios of principle stresses in the confinement process, on peak and residual (converging to frictional behaviour in the CSL) affect undrained strengths. Full symbols correspond to anisotropically consolidated specimens and empty symbols to isotropically consolidated specimens.

3.5.4 Stress induced extension paths implication on CSL and Undrained Strength on the onset of Instability

Figure 16 presents the extension triaxial test results conducted on soil Type 4. These tests were carried out for both drained and undrained conditions under anisotropic consolidation (i.e. $K = 0.5$) in a Bishop-Wesley triaxial cell to simulate in situ loading conditions under stress-paths different from the conventional axial compression loading. The stress paths hereby conducted were adopted to study the expected induced lateral stresses under a potential instabilization of an earth mass after the triggering of a loss of strength (such as the illustrated in Figure 16).

To ensure uniform shearing, a v-ring connecting the top platen and the top cap was employed before the consolidation phase, minimising misalignment between the loading ram piston and the specimen axis (Cordeiro et al., 2022; Viana da Fonseca et al., 2023). From the Figure 17, it can be observed that the soil did not achieve very large strains. The "necking" effect in the extension triaxial results of soil Type 4, is illustrated and is expressed in the q:ε_a and Δ_u:ε_a curves, which exhibit a similar and parallel tendency, stabilising after ε_a of -6%. The stabilisation of q:ε_a, Δ_u:ε_a and ε_v:ε_a facilitated the definition of CSL in the extension path.

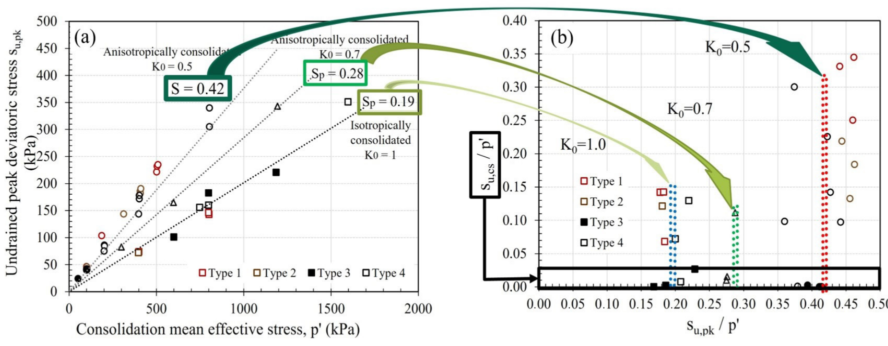

Figure 15. Effect of consolidation path on the peak (a) and residual (b) undrained strength values.

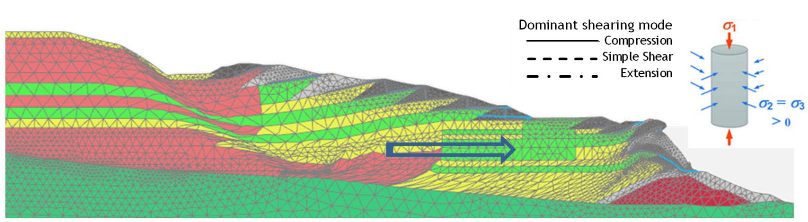

Figure 16. Dominant extension stress-strain path by lateral movement (adapted from Arroyo & Gens, 2021).

Figure 18 presents the stress paths used to infer the CSL of soil Type 4 from extension triaxial test results. The CSL projection in the q:p' invariant space defines a strength parameter M_{te} equal to 1.034. Therefore, by transforming M_{te} into the critical state angle resulted in a mostly unique value of 38.6°. This value is slightly higher than the value obtained for compression triaxial tests, in line with Salvatore et al. (2017).

The CSL inferred from extension triaxial tests in the e:log p' invariant space for soil Type 4 is defined by a power law relationship (i.e. A = 1.084, B = 0.031 and C = 0.611) while p' is the mean effective stress and p_{ref} is the reference stress condition assumed generally 100 kPa. Particle size distribution analysis of specimens tested at 800 kPa and 1600 kPa of confining stress were evaluated, showing that no particle breakage occurred. Consequently, the curvature of CSL is mainly caused by soil instability, which induces a higher susceptibility to flow liquefaction in this soil.

These results indicate that the uniqueness of CSL for compression and extension stress paths is debatable, as stated in other studies (Yamamuro & Lade, 1996; Riemer & Seed, 1997; Fotovvat & Sadrekarimi, 2022; Wagner et al., 2023). It should be remarked that in these more recent works some critical options may be identified. Fotovvat & Sadrekarimi (2022) are taking the phase transformation point to be the CSL, which is not correct, and Wagner et al. (2023) used only dense extension tests, which are likely to develop early localization with strong influence in the results. In drained conditions the uniqueness of CSL is more acceptable in compression and extension stress-paths for granular materials with stable particle distribution and morphology, as far as necessary specific imaging treatment of the shearing areas on extension tests are used, as proved by Salvatore et al. (2017) and Becker et al. (2021), using X-Ray tomography and photogrammetry, respectively.

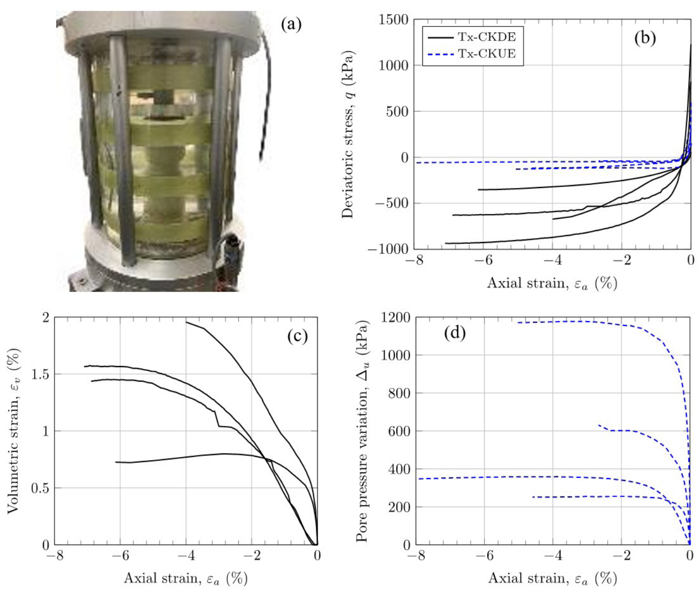

Figure 17. Triaxial test results in extension by lateral compression: (a) necking; (b) stress–strain behaviour; (c) change of volumetric strain in drained; (d) pore-pressure variation in undrained conditions.

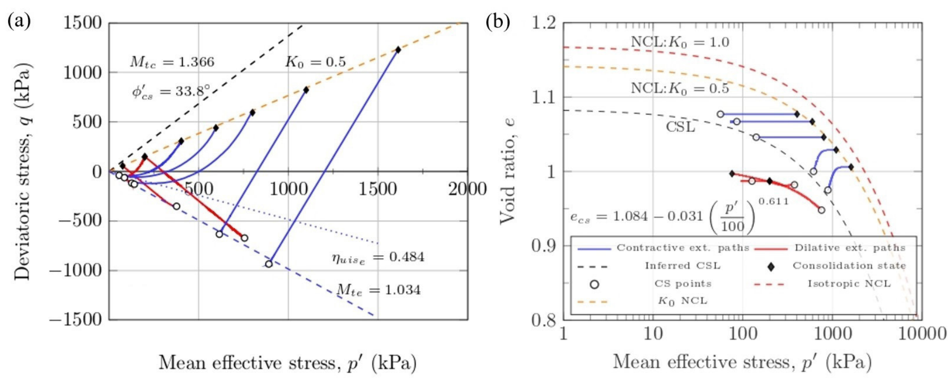

Figure 18. Inferred CSL from extension triaxial tests: (a) q:p' invariant space; (b) e:ln p' invariant space (adapted from Delgado et al., 2025). **Note:** red tests results correspond to dense conditions, where necking is aggravated.

In the analyses that the tests it was shown a clear trend of a unique CSL in compression and extension as recently well sated by Fanni et al. (2025) for gold ore tailings. They took significant effort to consider localisation behaviour of the samples in extension, as in the current work hereby described with iron ore tailings from Dam 1.

However unsurprisingly, as it is the case of loading increment in lateral compression generating an extension shearing, the maximum values of deviatoric undrained deviatoric stresses after inversion of principal stresses (therefore the mobilized undrained shear strength) are much lower than the maximum values caused during compression shearing. These effect of inversion of the principal effective stresses with in extension path, and the axial stress becomes the minor effective stress, while horizontal stresses become the higher redistribution generated large zones with ruptures in the sloping ground masses. Soil anisotropy is typically defined by two components, inherent or induced anisotropy. The at initial – “at rest” - stress state, with consequences in structure (at macro to micro levels with consequences on fabric - arrangements of particles and voids - and bonding between particles) following the stress-strain history, and the subsequent loading stress paths, conditioned by the Lode angle (θ) (Lode, 1926) or the intermediate principal stress ratio (b) (Habib, 1953), or direction of the major principal stress relative to the vertical axis (α) and by the pre-shearing stress ratio (Kc). Works on geomaterials prepared in loose and dense states have clearly indicated the dependency of the peak friction ratio (η_{pk} or η_{IL}) and M on the Lode angle θ, such the very early work from Matsuoka & Nakai (1974). The testing consisted of drained/undrained TC (i.e. TC: $\theta = 30°$ or $b = 0$, $\alpha = 0°$) and extension testing (i.e. TE: $\theta = -30°$ or $b = 1$, $\alpha = 90°$).

In spite of the scarce number of high quality advanced testing on tailings to investigate the mechanical behaviour, specially the effect of anisotropy on instability of tailings, recent works in Western Australia University resumed in Fanni et al. (2025) allowed to resume as follows the mainstreams of the drained and undrained behaviour of sandy silt gold tailings under general multiaxial conditions (sic): (i) the CSL in the compression plane does not depend on θ or on the stress path; (b) the stress-dilatancy is dependent on θ while the effect of θ on state-dilatancy is minor; (c) the undrained yield strength of LMT was found not to depend significantly on the state parameter (ψ), but it was significantly affected by the stress path followed during consolidation and subsequent shear, for example, by the pre-shearing stress ratio, stress-reversal loading, θ and α. The results demonstrate the contribution of the initial shear stress and evolving anisotropy on the undrained strength of the gold tailings in a loose state.

Figure 19 shows the onset of instability on undrained compression and extension tests conducted on loose samples in type 4 iron ore tailings hereby described anisotropically consolidated, i.e. $K = 0.5$, represented in the q:p' invariant space. These results

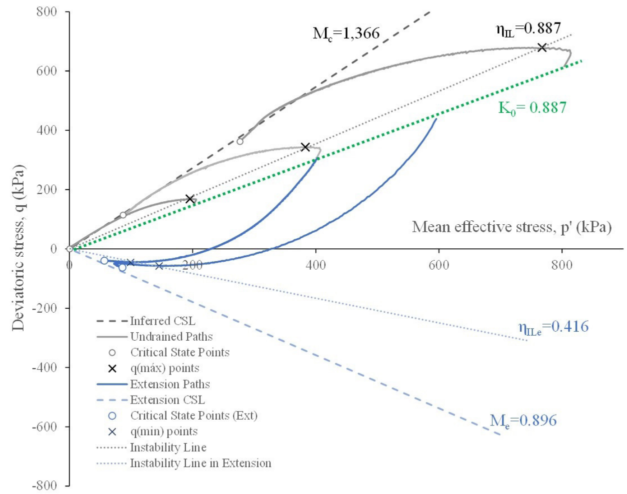

Figure 19. Onset of instability on undrained compression and extension tests.

allowed for a derivation of a linear tendency describing the instability for both compression (η_{pk}) and extension (η_{pke}) paths. Particularly, η_{pk} is equal to 0.416, which corresponds to half of the compression stress ratio η_{pk}. This finding implies that the instability region in extension conditions is narrower than in compression conditions, as anticipated due to the inversion of principal stresses during the extension path.

By interpreting the undrained softening underlying the flow liquefaction phenomenon using the CSSM framework, Fanni et al. (2025) have considered the non-linear CSL observed in the e:log p' invariant space was used to interpret the intrinsic undrained response of tailings, defined by the instability locus. The effect of the isotropic and anisotropic consolidation and stress paths under different Lode angle (θ) values was analysed, as well as between compression and extension triaxial tests

The undrained yield strength (instability locus) of tailings depends mainly on consolidation stress conditions rather than the angle ψ. Initial shear stress and anisotropy significantly influence yield strength: positive when shearing without stress reversal, negative otherwise. Under typical below-slope conditions, higher static stresses increase yield strength, likely due to particle arrangements aligned with the load, causing a shift or rotation of the yield surface in the loading direction.

3.5.5 Brittleness and rigidity ratios to look at potential sensitivity of granular soils

The brittleness index I_B proposed by Bishop (1967) is a soil parameter that expresses the likelihood of a material being involved in a flow slide. It is defined by:

$$I_B = \frac{s_{u,pk} - s_{u,cs}}{s_{u,pk}} \cdot 100\% \tag{5}$$

where $s_{u,cs}$ refers to the critical state undrained strength on the lowest value of undrained (also commonly named residual, $s_{u,res}$, hereby renamed as $s_{u,cs}$, since it may be associated to the convergence to a frictional Critical State). As expected, the brittleness index decreases with the increasing compaction and pre-consolidation pressures.

I_B index for most of the undrained tests executed in these tailings, even with no preloading or over consolidation, was generally higher than 50%, implying a brittle behaviour of the soil. The elastic shear modulus (also designated as initial, G_0, or maximum, G_{max}) is an important soil property since it defines the soil stiffness at very low strain levels, particularly when normalized by mean effective confinement stress. This ratio is associated to a singular interaction between the particles that create a structure with micropores formed by finer particles (interlocked –or bonded - cementing bridges), arranged around meso/macro pores associated to coarser particles. This creates a transient fabric that can sustain a stiff stress-path for the early stages of induced stresses that diminish the mean effective stress, and at a specific stress ratio ($\eta_{pk}=q_{pk}/P'_{pk}$)$\eta_{pk}=q_{pk}/P'_{pk}$) drops steadily to very low deviatoric stresses under a instable flow process until it regains a steady frictional critical ratio ($M=q_{(cs\,;\,res}/P'_{cs}\ s_{u(cs;res)}\ /P'_{cs}$ $M=q_{(cs\,;\,res}/P'_{cs}\ s_{u(cs;res)}\ /P'_{cs}$).

This relation between the elastic shear modulus (also designated as initial, G_{max}) and the peak deviatoric stress (q_{pk}) q_{pk}) or half of its ($s_{\mathrm{u,\,pk}}s_{\mathrm{u,\,pk}}$) is called the Rigidity Index (I_R) and can be inversely associated to I_B, therefore highest values of I_R are associated to more pronounced metastable behaviour, as describe by many authors in different material.

A more comprehensive analyses of the advantages of using this approach is described in Soares et al. (2023). A large set of undrained compression triaxial tests was carried out on different types of cohesionless soils, from sands to silty-sands and silts. Shear wave velocity measurements were carried out alongside. These tests exhibit distinct state transitions ranging from flow liquefaction to strain softening or strain hardening. With the purpose of defining a framework to assess soil liquefaction, it was found that the ratio between the shear wave velocity (V_{S0}) and the peak undrained deviatoric stress, q_{pk}, V_{S0}/q_{pk}, can be accurately used to define a boundary between liquefaction and strain hardening for sands, and between strain softening and strain hardening for silty-sands and silts. Since this ratio is a function of the tested material, the prediction of these boundaries can be made as a function of soil grading, namely via the coefficient of uniformity, C_U. Despite not being regarded as a strong geomechanical parameter, C_U is easily determined from a grain-size distribution test and it has an empirically proven correlation with critical state parameters.

In the lab the evaluation of that maximum (initial/elastic) distortional stiffness it can be achieved with bender element testing, directly determining seismic wave velocities by the classical equations of isotropic elasticity:

$$G_{max} = \rho \cdot V_s^2 \tag{6}$$

where ρ is the bulk density of the soil and V_S is the velocity of the shear wave. G_{max} can be related to mean effective stress (p'), being commonly expressed as:

$$G_{max} = G_{ref}\left(\frac{p'}{p_{ref}}\right)^n \tag{7}$$

where G_{ref} is a reference shear modulus at the reference stress level p_{ref} of 100 kPa and n is the exponent controlling the evolution of G_{max}.

The obtained results indicate a higher stress-dependency for Type 1 soil in Brumadinho Dam 1 three tailings clusters analysed in Vian ada Fonseca et al. (2022), expressed by the higher stress exponent, n, in equation (7), is typically observed in soils with a weaker induced or inherent structure/fabric. It was observed that the coarser/heavier blackish soil exhibits lower stress-dependency. These results indicate a high stress-dependency of Vs, expressed by the exponent of the laws in Figure 20, being even more evident (higher) in the coarser and heavier tail ("black"), which is typically observed in soils with a weaker fabric or inherent cementation (as very clearly resumed by Santamarina, 2003, and Cho et al., 2006). In Situ Seismic Dilatometer Tests (SDMT) in Brumadinho Dam 1 2018 campaign allowed the determination of shear wave velocity, Vs, every 0.5 m of advance using a down-hole true-interval method (one meter). It is clear from Figure 20b that there is a trend to fit with the results in undisturbed samples (blocks), and this trend shows that cementation/bonding between particles is incipient in these tailings, which was confirmed microscopically.

Figure 21 presents a comparison between V_s values of the three types of tailings, tested in remoulded conditions, and in an undisturbed sample, prepared from a block directly extracted in the remains undisturbed masses in the post-morten resservoir. The two Elastic Stiffness Vs Consolidation mean effective stresses laws in remoulded conditions denote a slight influence of induced fabric, while the intact block specimen having a similar n value, but the constant A parameter three times higher!

3.5.6 The dependency of the instability line / locus (η_{IL} or η_{pk}) with the state parameter

Since early studies (Chu et al., 2003 and Chu & Wanatowski, 2008) on CIU triaxial and plane strain tests on sands the dependency of the slope instability lines (η_{IL}) in the deviatoric stress (q) versus mean normal effective stress (p'), with the variation of void ratio, but not with the consolidation stress ratio ($\sigma'_h/\sigma'_v \cong K_0$), as expressed in Figure 22.

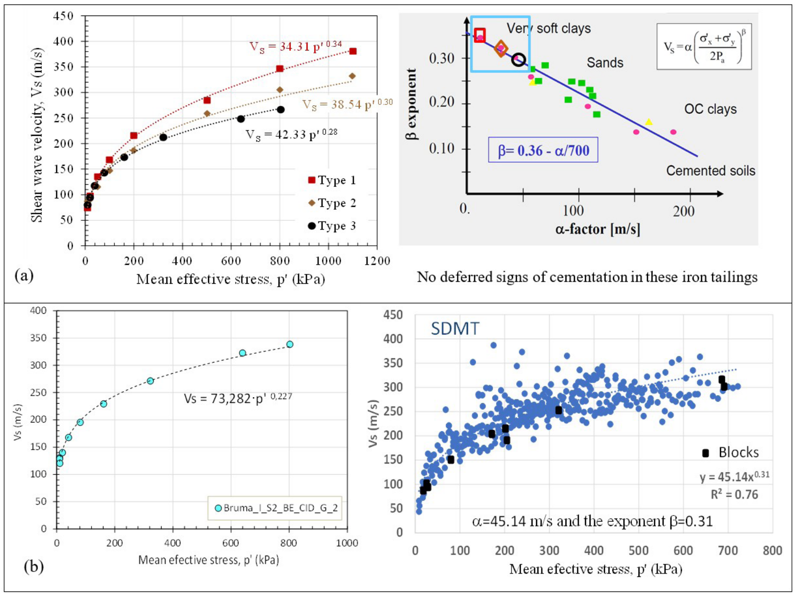

Figure 20. Evolution of shear wave velocities (V_s) as a function of mean effective stress for the three types of tailings: (a) results in reconstituted samples in the three types, 1,2, and 3; (b) results from the evolution of *Vs* with *p'* in a block undisturbed sample and four other block samples plotted over *Vs* situ values (SDMT).

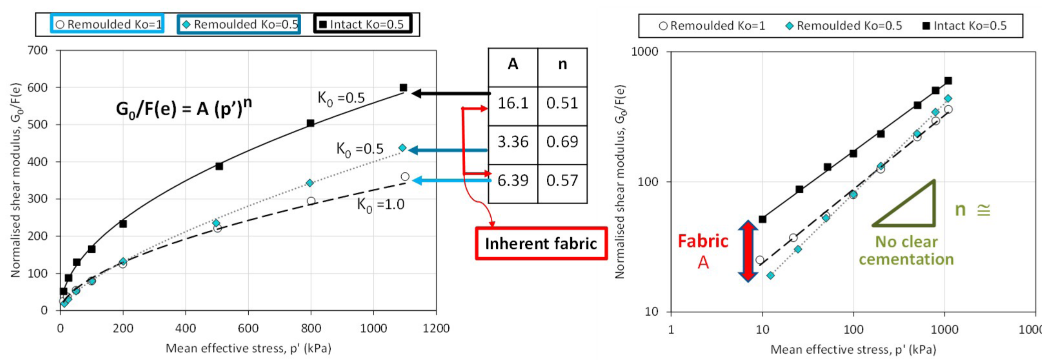

Figure 21. Evolution of shear wave velocities as a function of mean effective stress for the three types of tailings.

Besenzon (2024) has obtained similar results in the tests carried in the geotechnical laboratory of FEUP, with the experimental results published in Viana da Fonseca et al. (2022), and the results obtained with CASM model explore the effect of consolidation history on undrained instability. To this end, a series of triaxial tests were simulated using the same constitutive model parameters previously employed for soil types 1 and 2. The results suggest that CASM can qualitatively capture the effects of varying consolidation paths on undrained instability (as presented in Figure 22c).

Chu et al. (2012) suggest that the instability line (I_L) is not unique for a specific soil but is highly dependent on the initial void ratio or, better, the initial state parameter ($\psi = e_0 - e_{cs}$, for the same p'). Furthermore, these tests revealed that the I_L slope remains constant once the state parameter surpasses a specific threshold. In Figure 23 numerical analyses with CASM (Clay and Sand Model) calibrated parameters from Dam 1 tailings (types 1 and 2) and conducted by Besenzon (2024), with the reference to experimental data, have proved this trend.

It is evident that the instability line remains unchanged until the state parameter attains a specific value, such as around 0.025 in the simulation of soil type 1 (red dashed line). Once this value is exceeded, the instability line begins start to ascend until it intersects the CSL. The area spanning from the lower instability line to the failure line is identified as the zone of potential instability (Lade, 1992, 1993). Consequently, the stability of a specimen within this zone is closely linked to its state parameter.

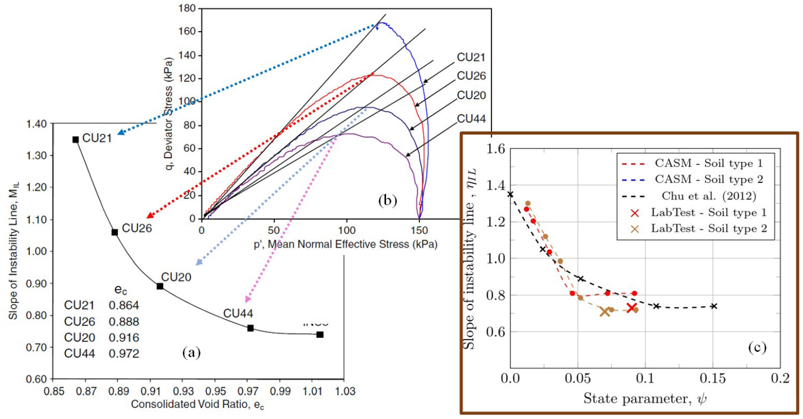

Figure 22. (a) Dependence of I_L on the void ratio of sand; (b) its variation with void ratio (modified from Chu et al., 2012); (c) Variation of η_{IL} with the state parameter in B1 soil type 1 and 2 (Besenzon, 2024).

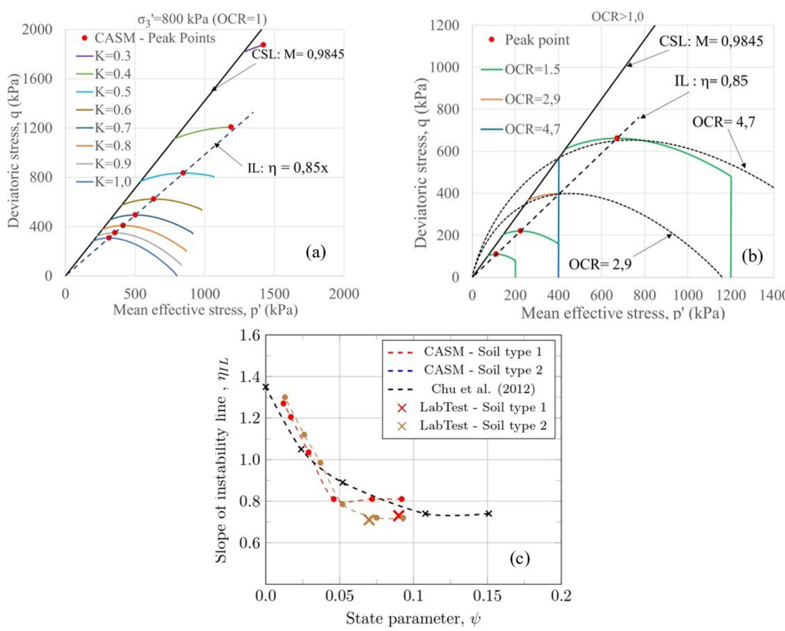

Figure 23. (a) and (b): Illustration of the evolution of undrained stress paths simulated in CASM for soil type 1; (c) variation of η_{IL} with the state parameter in soil type 1 and 2 (Besenzon, 2024).

3.5.7 The post-peak strength / residual / "liquefied"

Residual strength (q_{res}), or more specifically the normalized residual or post-liquefaction/instabilization undrained shear strength ($s_{u' res}/\sigma'_{vo}$ or $s_{u' cs}/\sigma'_{vo}$) is very difficult to identify, particularly if any partially drained loading redistributes void due to diffusion of excess pore pressures, local loosening causing instability.

However, what is very clear today is that the determination of the residual post-peak (post-yield) residual or liquefied (a term that can be misleading, since in fact is a post partial liquefaction frictional strength, is very difficult to determine in laboratory (Chu & Wanatowski, 2014). This is more pronounced in load-controlled undrained tests where the rapid drop of the stress-path after peak doesn't allow for a net definition of the intersection of the Critical State Line (on the onset of a flow instability in a transient "pseudo"-liquefaction). But, it is also difficult accept as undiscussable the value that is more clearly defined in a deformation-controlled undrained tests, both in natural sandy/silty soils or tailings. This control of strains is realistic in permeable materials where partial drained conditions develop, when this phenomenon of softening can also occur. Therefore, it is expected that results obtained under a deformation-controlled loading condition (as illustrated in Figure 24) and a load-controlled loading condition leed to different post-peak (residual) behaviour, which can be attributed to very different stress – strain - and pore pressures homogeneous distributions, due to geometric/border distinct conditions.

Other well recognized approaches to define the residual post-peak after "instability/liquefaction" have been recognized as potentially more representative is the numerical back-analyses with advanced models of well fundament dams / piles collapse case histories (Olson & Stark, 2002). This was also done recently taking advantage of the results obtained in the numerical analyses of Brumadinho Dam 1 failure using "CASM-Liq" model and with the constitutive parameters defined from the already described advance laboratory test conducted in FEUP. The simulation of the long time (more than 40 years) construction of the structure and the consideration of possible triggering actions that defined the failure mechanism, fitting clearly that identified by video imaging treatment, was reported the CIMNE/FEUP Panel (Arroyo & Gens, 2021). The evaluation of the evolution of $(q/2)/\sigma'_{v0}$ in successive phases of the actions revealed in that numerical analyses pointed out to a value of the residual strength along the failure zone corresponding to a very low ratio of $(s_{u,res})/\sigma'_{v0}$ (0.02 – 0.04), as represented in Figure 25.

3.5.8 Creep/viscous behaviour of non-plastic tailings

Some discussion has been lasting since the public disseminations of the two expert panels (EPR - Robertson et al., 2019, and CIMNE - Arroyo & Gens, 2021) that investigated the possible causes of the failure the Dam 1, on the possibility of creep being a cause of the liquefaction mechanism developed. While the EPR defend that this may be caused by bonding of the tailing particles due to iron oxides, which endow extra brittleness and consequently superior instability. Microscopy was presented in remoulded samples, which is not the most significant condition for that identification, and visible in triaxial response, drained or undrained. An interpretation of cone penetration test (CPTu) and shear wave velocity V_s data using empirical criteria is claimed to show further evidence of microstructure. This has been with tests conducted in the geotechnical laboratory of FEUP as described in what follows. Creep can occur in drained and undrained conditions. Drained creep effects in soils are due to the passage of time without any observed pore pressure or effective stress changes and are usually described under the term "aging". Undrained creep in soils is usually associated with clays, which remain undrained while creeping under a constant load. Clays subject to constant shear stress under undrained condition may show significant creep strain accompanied by increases in pore pressure. A similar effect is noted when clays are sheared undrained at different strain rates (Arroyo & Gens, 2021). The undrained strength observed

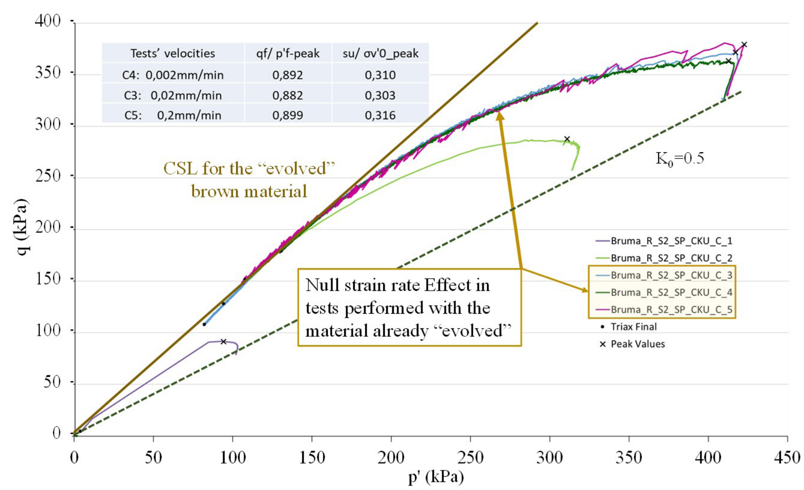

Figure 24. Undrained stress-paths under strain control from K_0=0.5 (two tailings from Córrego de Feijão mine).

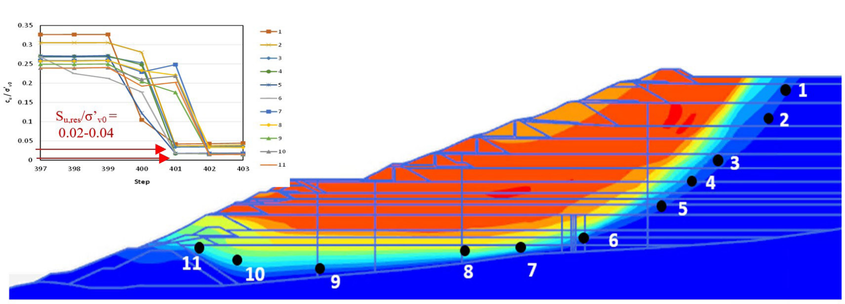

Figure 25. Values of $(s_{u,res})$ / σ'_{v0} on the sliding surface on the last step/phase before failure in the numerical analysis (reassessment of the calculations in Plaxis® with CASM).

reduces with strain rate, being accompanied by a significant raise in pore pressures as the strain rate reduces.

To evaluate creep behaviour, strain rate effects on the tailings were systematically measured in the different reconstituted materials using strain-rate controlled triaxial tests. For this effect, three triaxial specimens of each material (three classes above referred) under the same consolidation state (density and confining pressure) were sheared, in which the undrained strain rate was systematically varied in a magnitude order of 10% (0.2; 0.02 and 0.002 mm/min).

The tests results are presented in Figure 26. The observed effect is equivalent to a change in undrained strength of 2% per order of magnitude change in strain rate. This experimental result suggests that the magnitude of measured strain-rate effects on the tailings was always small and did not anticipate a large role for viscous effects (or “creep”) in the failure.

These results suggest that the magnitude of measured strain-rate effects on the tailings was always small and did not anticipate a large role for viscous effects (or “creep”) in failure. That result is well aligned with the expected behaviour of non-plastic granular materials (Mitchell & Soga, 2005). It is important to evaluate this sensitivity to a factor that may condition the equilibrium of the interparticle structure, which in the case of working with fabric induced in the preparation of the remoulded integer samples, should be, at least, compared with representative undisturbed samples where intra/interparticle structure (fabric and cementation), have unfavourable trends in terms at the potential of sensitivity (see section 3.5.5). In the case of the remould give less trend to the factor of structure, this issue can be neglectable in granular soils. If not, similar tests to as described should be done and analysed accordingly.

4. In situ tests: fundamental for modelling the behaviour of geotechnical structures

4.1 Materials selection CPTU clustering

Geotechnical characterization of the tailings that constituted a TSF, in particular a dam, has to give enough information to define prevalent homogenized clusters that could define zones (clusters) to conduct stability analyses or any other hydro-mechanical calculations for specific objectives (as different as the definitions of flow nets – therefore masses subjected to leaching - or the identification of zones of materials prone to cyclic liquefaction, as examples). This is crucial in numerical analyses to be conducted for the studies of eventual causes (“triggers”) of ruptures, which will not be discussed here. In fact, to obtain a credible computational model of the failure, but from a practical and effective point of view, a discretisation of limited clusters/block inside the deposited masses some hypothesis have to assumed: how many materials can fairly represent the complex distribution of tailings through the dam (heterogeneously distributed and strongly interlayered); and, how can sampling materials are compatible with the dominant soil behaviour types present along the dam (coarse to fine granular tailings, silty sands, mostly silts and even slimes).

This subject was initially addressed by analysing the fruitful data from several CPTu testing campaigns during the period from 2005 and 2018 (Figure 27). The soil behaviour type index *IcRW* = 2.60 proposed by Robertson & Wride (1998), normally used to separate fine from coarse material, may usually separate correctly mostly granular and mostly cohesive soils in natural deposits however, it is unclear if this value is also the best for tailings. In the studies of CIMNE (Arroyo & Gens, 2021) a different threshold for *IcRW* was established based on the drained and undrained response to CPTu tests, to a higher value of 2.85, optimising the fine and coarse behaviour type horizons.

It is decisive for any stability analyses to assume essential drained or undrained conditions, which are due in limit equilibrium analyses. For this a clear analysis of soils that respond in a drained manner to CPTu penetration is necessary. Permeability should be the key property to differentiate fine from coarse soils, and, as in B1 case, this was also correlated with important critical state properties. The easiest and more reliable undrained response to a CPTu shall be quantified by the normalised excess pore pressure index Bq (Figure 28).

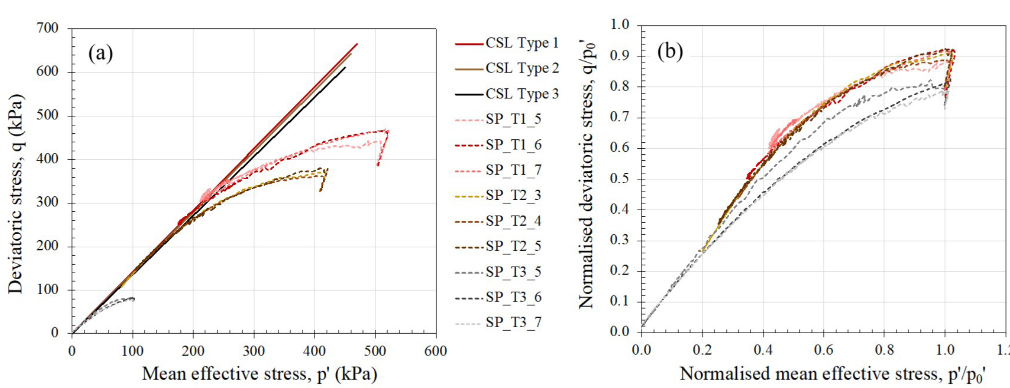

Figure 26. Assessment of stress-strain dependency on the different tailing types.

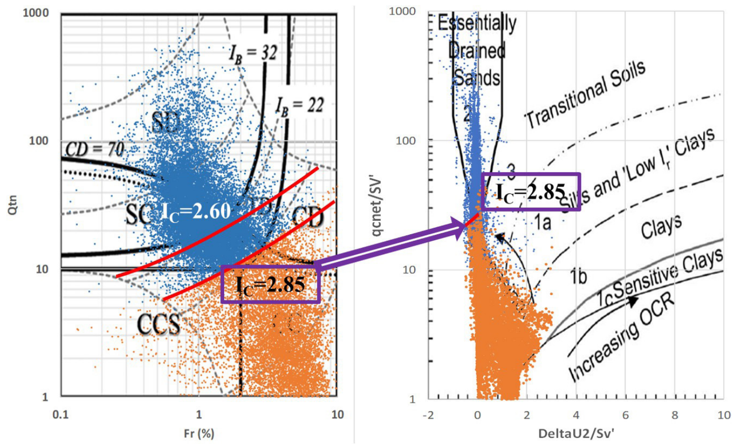

Figure 27. subdivision in clusters, in order to separate the fines and the coarse fractions, by the limit of SBT index Ic_{RW} = 2.85 was more effective (Ramirez Orbegoso, 2021).

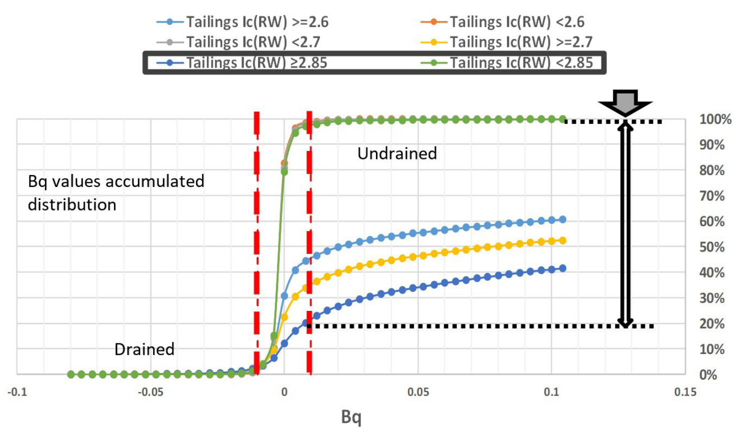

Figure 28. Separation of the tailings through different values of SBT index (*IcRW*). Red lines limit the region of essentially drained response to CPTu penetration from B_q analyses (CIMNE, 2021)

To model the materials each and all positioned in a ground model, Arroyo & Gens (2021) have reported the analyses to 38 CPTu, corresponding to around 1km and 37000 useful datapoints (90% on tailings). But in this study of the previous CPTU traces were very variable and appeared to be random, showing some consistency in terms of stages of the construction and even on the position of spigotting points. CPTu results showed that different deposition phases were often coincident with significant changes in mechanical response defining a spatial distribution of tailings within the dam, blocks were created accordingly (Figure 27).

The permeability limits fitted well with the evidence from the CPTu, with most dissipation tests at locations classified as "Fine" (*IcRW* > 2.85). When restricted to these "fine" materials the permeabilities from CPTu dissipation tests are almost all below 10^{-6} m/s.

These blocks correspond to a specific section, raising and alignment of the dam and have some allocated data from the corresponding CPTu tests. For practical reasons, only a limited number of material types can be used in the numerical simulation. Thus, CIMNE decided to use three different types of tailings to assign material properties to the different blocks in the model.

Three materials were idealised, covering all material distribution: Fine tailings (when the CPTu indicated a proportion of Fines Content, *FC*, equal or above 50%); Coarse tailings (when the CPTu indicated a proportion of *FC* equal or below 10%) and Mixture tailings (for CPTu *FC* between 10 and 50%). The objectiveness in the sampling campaigns was crucial to retrieve best "material models" in soil behaviour types.

FEUP investigated all remoulded/integral and intact/undisturbed samples obtained in the different sampling campaigns. From the physical properties (mainly particle size distribution, PSD and specific gravity, G_s) and the coloration of the materials found, it was selected a set of three ideal materials to be representative of different tailing materials within the dam identified in the CPTu analyses. The typological classes of soils were named as Type 1 for red fine tailing material collected on Site 1; Type 2 for the brown very fine material collected on Site 2; and Type 3 for the black granular material collected on Site 1.

The intact/undisturbed samples were not selected to constitute the numerical modelling as it is very difficult to pass from the specificities of this undisturbed stratified material to an extrapolation for a unified model of each of the constituents. The red/brownish material collected from Site 2 wasn't considered to be representative of the tailing's reservoir, far away from the rupture, showing a very erratic interlayered, and combination of physical characteristics of the soils under evaluation. The samples retrieved from Site 3-Local 4 were also not considered in the numerical modelling as they were too close to the embankment berm and further to the location of the initial failure surface. Nonetheless, after analysing the integral samples collected from Site 3-Local 1, the black coarser tailing was considered an ideal material

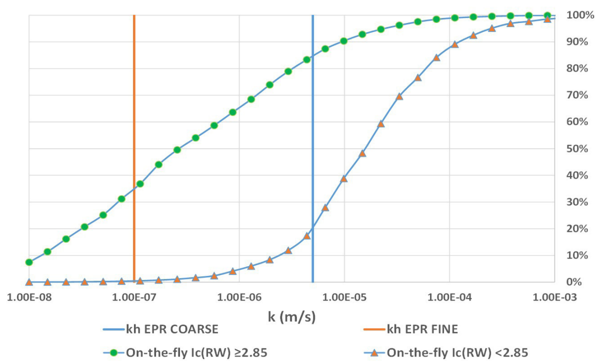

Figure 29. Values for "fines" interpreted by "on-the-fly" permeability are above those of dissipation tests (the method is not precise for very impermeable materials (above 10^{-6} m/s).

to be representative of different tailing materials within the dam, given its brittleness and proximity to the initial failure surface location. However, this material, named Type 4, was not included in the 2020 dam's modelling, as it was still being tested at the time of the computational analysis, due to its late arrival to FEUP (LabGEO). The mechanical characterization of tailing type for was then collected in an independent report, from which some results are being published.

This grouping into three typological groups would be later confirmed by the results obtained in laboratory tests for the determination of hydraulic conductivity (permeability), volumetric compressibility in confined conditions (either in isotropic loading or in oedometric loading –unidirectional) and shear strength resistance, in diversified conditions that would necessarily have to be developed in a work of such complexity, where different drainage conditions (total drained – or inhibited – not drained) and loading paths were conducted.

It is important to refer that excluding points where there was no excess pore pressure, there were still left more than 7000 tailing points classified as "fine" and 4400 classified as "coarse". The following formulation for the evaluation of hydraulic conductivity from piezocone on-the-fly (Monforte et al., 2018) was used:

$$k = \frac{v \cdot d_c \cdot \gamma_w}{\sigma'_{v0}} \cdot \frac{\lambda}{\left(1+e_0\right)\cdot V_{50}} \left(\frac{\Delta u_{ref}}{\Delta u} - 1\right)^{1/c} \quad (8)$$

In this case, five parameters are involved (c, V_{50}, Δu_{ref} or a, λ, e_0). Two parameters (λ, e_0) may be independently measured.

In Figure 29, it is noticeable that for "coarse" points, where the "on-the-fly" permeability is more reliable, the values obtained are almost all above 10^{-6} m/s, in good agreement with G-PFEM simulation.

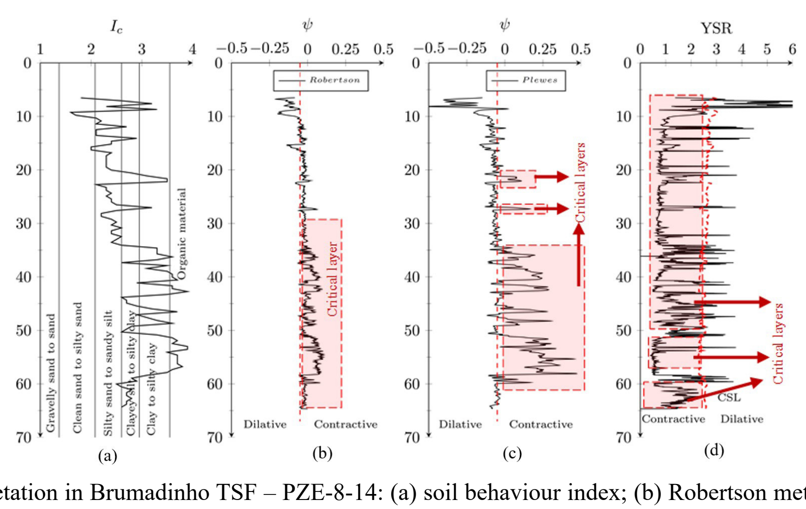

Figure 30. CPTu interpretation in Brumadinho TSF – PZE-8-14: (a) soil behaviour index; (b) Robertson method; (c) Plewes method; (d) Mayne method.

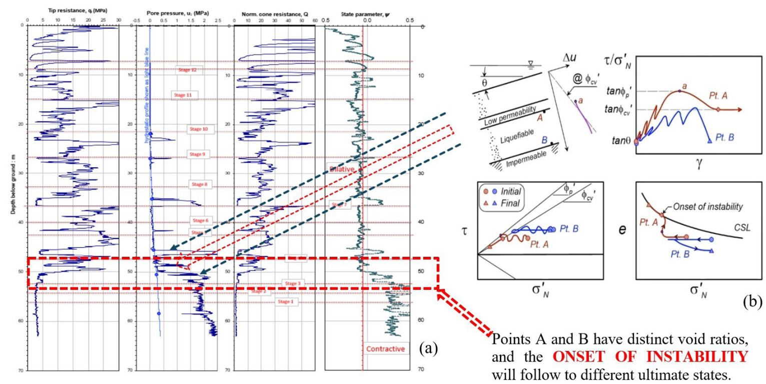

Figure 31. (a) Triggering of Instability in layered systems with liquefiable layer overlain/underlain by low permeability soft layer(s) (Boulanger, 2022; Iai & Tobita, 2022); (b) system response in the zone of the borehole associated to the failure of B1 dam as an explanation of the unexpected triggering (adapted from Kulasingam et al., 2004).

4.2 State parameter and yield-stress-ratio approaches

4.2.1 Flow liquefaction susceptibility of iron ore mining tailings from CPTu data

Susceptibility to liquefaction is typically evaluated with the CPTu by estimating the state parameter (ψ). This parameter allows estimating the contractive or dilative behaviour combining density and stress level under critical state soil mechanics (CSSM) framework. Soils with soil behaviour index (*Ic*) less than 2.60 (or other threshold has discussed above) and contractive behaviour (ψ > -0.05) are more susceptible to trigger liquefaction. Contractive and dilative behaviour can be also evaluated by alternative approaches, such as yield-stress-ratio (YSR). YSR values under a threshold value also given by CSSM indicate a contractive behaviour, while values above indicate dilative behaviour. CPTu data from a Brazilian mine tailing dams, were categorised in a paper of Viana da Fonseca et al. (2021) in their states in terms of contractive/dilative behaviour to assess the liquefaction susceptibility of these complex materials. Although the two procedures applied have similar basis, the results obtained have similar basis, but the results obtained were not always coincident (Figure 30).

Soils with in situ ψ < -0.05 or *YSR* < 3 revealed contractive behaviour and high susceptibility for trigger liquefaction. The results of this paper showed differences between the profiles delineating with the addressed methods. These differences were attributed to the intrinsic variability of soil profiles, evidenced through interbedded layers composed of soil mixtures. Besides, these differences were associated with uncertainties in the input parameters used in the computation of Plewes and *YSR* methods, which depend on laboratory data. Therefore, the authors recommended further studies in the laboratory to characterise the physical and critical state parameters of iron tailings, providing a reliable connection between ψ obtained through in situ and laboratory testing. Such a connection will allow defining the method explored in this paper to better delineating the contractive/dilative behaviour profile from CPTu data. Some evolution has been observed on the methods, since the recent advancements in numerical has completed approximations based on cavity expansion in simulating cone penetration, as described in a recent PhD thesis in the University of Porto (Besenzon, 2024). From these methods possible realistic cone simulations using various techniques like Shuttle & Jefferies (2016), Monforte et al. (2021, 2023), Pezeshki & Ahmadi (2021) were applied to two of the boreholes in Dam 1 and the results present some differences discussed in the thesis.

4.3 Reproduction of complex intermediate behaviour with advanced procedure: system response in field

Recently, several relevant works have been focuses on the importance of the system response of interlayer deposits natural or anthropic (Boulanger, 2022). As described in this keynote lecture in ICSMGE in Sydney, 2022, the mechanisms developed when excess pore pressures in a specific contractile granular soil can diffuse imposing partially drained conditions towards other layers less permeable, that is, inducing local densification (net outflow) and local loosening (net inflow) in deposits with lower- permeability interlayers. This process is illustrated schematically for an infinite slope in Figure 31 (adapted from Kulasingam et al., 2004) where an upward seepage driven by excess pore pressure gradients causes the sand just below the low permeability lens to loosen sufficiently to conduct the slope to an onset of instability. The response of soils to partially drained conditions with imposed volumetric strain paths (net outflow/inflow) during monotonic or cyclic loading have been studied experimentally by: Boulanger & Truman (1996), Vaid & Eliadorani (1998, 2000), Sento et al. (2004), and Yoshimine et al. (2006) - all cited by Boulanger (2022). Numerically, Kamai & Boulanger (2013), have simulated the effects of partial drainage on monotonic, cyclic, and post-cyclic responses of liquefied sand. In the same line a recent case was analysed by Iai (2021) and Iai & Tobita (2022) related to the process of soil liquefaction in Petobo Housing Complex which has induced a lateral spreading of almost 1km in an average slope of 2.3º.

4.4 Effective stress–state fully coupled analyses

A brief note on the increasing recognized importance of the coupled stress–deformation analyses in numerical techniques to study the realistic possibility of static liquefaction events, highly dependent not only in state parameters concepts but also and essentially in the capacity of null/partial/full dissipation of the transient excess pore pressure regime induced by any triggering factors. The use of steady state flow nets, even carefully defined with the knowledge of the permeabilities in the mass, the internal and external contours and calibrated with monitored piezometric levels, are not sufficient, since the stress-strain calculations, integration advanced constitutive models, have to comply for the real effective stress evolution during the loading. This being highly dependent of hydraulic conductivity, in situ tests are determinant, being the dissipation tests in CPTu logs the most interesting - efficient and reliable - method.

Since classical methods of stability analysis based on limit equilibrium, are poorly adapted to incorporate any of these transient behaviours, as well as the post-peak evolution and brittleness of these more or less sensitive materials, the use of commercial numerical platforms is steadily increasing, in industrial practice. Numerical analysis prove that a large static liquefaction failure might be triggered by unexpected factors (extrusion paths in erosion – ex.: Mánica et al., 2022).

Constitutive models selected to represent tailings behaviour is a key element in this kind of analyses. Critical state soil mechanics offers a clear framework to understand static liquefaction (Jefferies & Been, 2016) and formulate constitutive models that reproduce this behaviour. This approach was pioneered by the NorSand model (Jefferies and Davies, 1993), updated recently and was employed to clarify the failure mechanism in the case of Fundão (Morgenstern et al., 2015). However, Robertson et al. (2019) had to abandon Nor-Sand numerical analyses of the B1 failure because of numerical instabilities. Recent back-analysis TSF failures were successful, Cadia (Jefferies et al., 2019) or Tar Island (Shuttle et al., 2023).

More recently, apart of B1, CASM - Clay and Sand Model- a model based on critical state concepts able to represent static liquefaction, was used to analyse the failure of the Merriespruit tailings dam, which took place in South Africa in 1994, and was instrumental in the recognition of how widespread liquefaction can jeopardize saturated tailings (Mánica et al., 2022). This year an interesting comparison of the performance of these two models has been published in the proceedings of 19th ECSMGE in Lisbon (Laera et al., 2024).

The model formulation is elaborated to show that all required inputs can be related to familiar concepts such as the critical state line, the state parameter, the normalized undrained peak strength, or the coefficient of earth pressure at rest. This is considered an important factor for the good interpretation of that failure.

5. Conclusions

A strong assumption comes from the experience of several, some very recent, case-histories of catastrophic failures of tailing dams (mainly upstream constructed) or under compacted piles, which are storing loose, saturated and poorly drained tailings and therefore were highly susceptible to liquefaction. This was confirmed with several studies of the case of Dam 1 of “Côrrego de Feijão Mine”, suddenly failed on January 25th of 2019 close to Brumadinho Village in Minas Gerais (Brazil). The author of this lecture has collaborated in one of these analyses and decide to share some of the findings with the purpose of drawing attention to the importance of investing in laboratory and in situ tests and following the most modern and adjusted practices, as well as being rigorous in the interpretation of the results obtained, which is not always easy.

Sufficiently very detailed zonation is mandatory, taking into consideration the hydro-mechanical properties of distinct cluster (zones) on these very large volumes of more or less sensitive/fragile geomaterials and a thorough and representative set of parameters to feed the now available complex constitutive models to run numerical calculations that permit a comprehensive simulation of the rapid failure of these structures. This needs to consider the “ADN” of these materials (physical and chemical constitution, mineralogic-morphologic particles facies) and state conditions (void ratios and fabric/cementation if any), which has defined those hydro-mechanical indices that have conducted to contractile / dilatant (or critical) behaviour zones when actions induce drained, undrained or partially drained loading actions. This process was well detailed in the referred report and it went far beyond current practices of simplified hardening or softening evolution in the stress-strain paths. The reproduction of the behaviors of brittle and metastable materials cannot be done using convention elasto-plastic models.

These iron ore tailings Critical States Lines (CSL) in the stress state (q-p’) are not significantly affected by high pressures induced in virgin stress paths, or after preconsolidation, while in the space of void ratio (e) versus p’ there is a change in shape, increasing nonlinearity in sequential loading, after the preconsolidation CSL will translate down. This behaviour may be associated to particles breakage and/or change in morphology. When the percentage of iron breakage is low, the main factor seems to be the roughness of the iron particles, while with less iron particles the evolution is due to the hardness of the parent rock. Roughness is as key factor in these iron particles as observed in SEM images in

Brumadinho tailings (Viana da Fonseca et al., 2022), but new techniques (Guida et al., 2017) based on fractal analyses are promising to incorporate this in the near future. This evolutive behaviour has to be dealt assertively, as it has implications with the options in extracting undisturbed or integer simples and the procedures adapted for preparation of representative reconstituted/remoulded specimens. From the more recent works results, which were included in this text during these last years (June 2022-present), it is mostly proved that, if the particles do not significantly evolve in terms of size and morphology, the critical state loci, defined in both q:p' and e:log p' invariant spaces, are unique on compression and extension in axisymmetric triaxial conditions.

From undrained tests, an instability or distinct instability lines was(were) inferred for each soil. In loose soil samples, linear relationship between the peak deviatoric strength and the mean effective stress at the peak was clear. This correlation enables the identification of the instability locus by drawing a straight line passing through the origin and the peak points of undrained stress paths. Analysis of stress-induced anisotropy in undrained yield and ultimate shear strengths in brittle loose silty iron ore tailings and the experimental results showed that stress-induced anisotropy has negligible effects on the instability locus of the studied tailings, if the direction of the stress paths are concomitant with the direction of consolidation path, meaning that on the invariant space q-p', the Instability Line ratio $= s_{u,pk} / p'_o$ is constant in spite of the K value (different consolidation conditions). This is a consequence of inherent of the particles' organisation (structure / fabric) or the spatial variations in local void ratios in loose material. The importance of anisotropy of collapse potential and of load-controlled rather that strain-controlled shearing was recognized by Hight (2024). However, the undrained strength ratio $S = s_{u,pk} / \sigma'_{vo}$ can represent well the variation of peak shear strength increases with changes in K, since S is strongly dependent of the anisotropy level. Therefore, the characterisation on these materials under different stress-path is fundamental for the calibration of constitutive models (e.g., CASM), which allows performing numerical studies to assess the stability of TSF.

The instability line remains unchanged until the state parameter attains a specific value, which is different for each soil. Once this value is exceeded, the instability line slope begins to increase until it intersects the CSL. The area spanning from the lower instability line to the failure line is identified as the zone of potential instability. Consequently, the stability of a specimen within this zone is closely linked to its state parameter.

Drained and undrained extension tests carried out on loose and dense anisotropically consolidated specimens to evaluate the tailings strength parameters in extension conditions, particularly when lateral stress increases in undrained or partially undrained conditions. Since commonly K_0 is less than one, this effect generates the inversion of the principal effective stresses during the extension path development aggravating the increase in porepressure. The extension stress ratio ($\eta_{pke} = q_{pke}/p'_{pke}$) at peak is reached at a very low compression stress ratio. This finding implies that the instability region in extension conditions is much narrower than in compression conditions. Recent publications have detailed this important factor to conditions of design and stability analyses of large earth structures, such the "dangerous" TSF.

The obvious necessity to consider an appropriate value for the residual strength (post-peak, τ_{res} or q_{res}), faces a serious limitation to identify it in lab, being some of the back analyses from case-histories of TSF collapses due to liquefaction triggers resulted in extreme low values of the overall ultimate resistance. A thorough evaluation of the evolution of $(q/2)/\sigma'_{v0}$ can (should) be, as much as possible, determined by numerical back-analyses with advanced models in well documented case-histories along the failure zone pointed. Some recent cases, like in Brumadinho Dam 1, have deduced very low ratios of normalized residual undrained strength, $S_{u,res}/\sigma'_{v0}$ (0.02–0.04).

In situ test were also covered, particularly the ones that are more capable to evaluate the hydro-mechanic properties of tailings structures, mainly in the decisive evaluation of the state conditions and consequently the more suitable parameters for advanced numerical analyses, which rely on those values for clustering (zonation) of the masses/ grounds. Without that and with no guarantee of the quality of prospective "undisturbed/intact" samples (extremely difficult and when possible, with complex systems – Gel Push Sampler, ground freezing followed by "gentle" coring), the modern in situ test equipment and interpretation methodologies are definitely compulsory. Some of these are mostly consensual, static come penetration tests (CPT/CPTU) and with seismic modulus (SCPTu, for determination of the seismic velocities, V_s and V_p, this one more rarely) and others that are steadily increasing in practice, like the seismic flat dilatometer DMT, or the cylindric pressuremeters. If the self-boring version, SBPT, is preferable but rarely available, the pre-bored Ménard type has improved a lot its flexibility and automatization and can help a lot in specific objectives, like the stress state at repos that varies a lot in the TSF retaining structures and reservoirs.

As referred the increasing capacity of the stress-strain coupled analyses in numerical codes to simulate the behaviour of these impactive structures, demand for a good zonation/clustering of distinct material, considering their behaviour as dilatant or contractile, from the state conditions, but also the permeability / hydraulic conductivity of the involved geotechnical materials under those sate conditions. These properties will condition the mobilizations of drained, undrained or partial drained responses that can give confidence for the stability evaluation or risk of instability. This hydraulic conductivity evaluation demand for, more than everything, very good options for the selection of modern in situ testing procedures and advanced interpretation methodologies, quite fruitful these days.

Acknowledgements

Acknowledgements are especially due to Prof. Marcos Arroyo and Prof. Antonio Gens, from CIMNE (UPC, Barcelona), who were directly involved in the definition the lab tests to define the necessary constitutive parameters for the models used in numerical analyses. This was done under a contract between CIMNE and VALE, SA, under a Term of Cooperation of Federal Public Prosecutor's Office, (MPF). FEUP, as partner of CIMNE, is recognized to VALE's collaboration in field and MPF support, namely in the sampling campaigns. For these we owe a special and personal acknowledge to dr. Sebastião Oliveira (MPF) and Ing. Leonardo Mesquita (PF) for their commitment in organizing, executing and illustrating the field work enabling the challenging work of collecting the representative samples and their transport to geotechnical laboratory of FEUP in safe conditions, as attested by VALE, SA, officers. A friendly recognition to Prof. Antonio Mendonça of the Federal University of Minas Gerais (BH), for a precious and continuous dedication to sampling and conditioning works, specially, in the 2nd and 3rd campaigns. The experimental work in FEUP hereby discussed is due to a fantastic team of collaborators, Daniela Coelho, David Bezenson, Diana Cordeiro, Fausto Molina, and the interpretation of the results and modelling also to António Fonseca and Sara Rios. A final acknowledgement to Dr. Marcelo Heidemann, from the Federal University of Santa Catarina, in Joinville, Brazil, for the suggestion for improvement of this written version of the lecture. Part of this was financially supported by the referred contract between CIMNE and Vale, and was also part of, as agreed with MPF, the research activities of CONSTRUCT– Institute of Research and Development (R&D) in Structures and Construction funded by national funds through the FCT/ MCTES (PIDDAC), with the Base Funding –UIDB/04708/2020.

Declaration of interest

The authors have no conflicts of interest to declare.

Authors' contributions

This paper was entirely produced by its unique author.

Data Availability

The datasets generated analyzed in the course of the current study are available from the corresponding author upon request.

Declaration of use of generative artificial intelligence

This work was prepared without the assistance of any generative artificial intelligence (GenAI) tools or services. All aspects of the manuscript were developed solely by the author, who take full responsibility for the content of this publication.

List of symbols and abbreviations

e	void ratio
e_0	initial void ratio
e_{cs}	critical state void ratio
e_{pk}	void ratio at the peak value of maximum dilation
I_c	soil behaviour type index
k	coefficient of hydraulic conductivity
η_{IL}	inclination of the Instability line ($\cong\eta_{pk}$)
η_{pk}	stress ratio at peak undrained strength line ($\cong\eta_{IL}$)
η_{pke}	stress ratio at peak undrained strength line ($\cong\eta_{ILe}$) in extension stress-path
p'	mean effective stress
p'_0	consolidation mean effective stress
p_{pk}	mean effective stress at the peak value of maximum dilation
q	deviatoric stress
q_{pk}	peak deviatoric stress
ASTM	American Society for Testing and Materials
B	Skempton's pore pressure coefficient
BE	Bender Elements
Bq	pore-pressure index
Cc	compressibility index
CIAEA	Extraordinary Independent Consulting Committee for Investigation
CIMNE	International Centre for Numerical Methods in Engineering
CO_2	Carbon Dioxide
CONSTRUCT-GEO	Geomechanics and numerical modelling of geotechnical structures
CPTu	Piezocone Penetration Test
Cr	recompressibility index
Cs	expansion index
CSL	Critical State Line
CSSM	Critical State Soil Mechanics
C_u	coefficient of uniformity
EOTSF	End-of-test soil freezing
EPR	Expert Panel Technical Report
FC	Fines Content
FEUP	Faculty of Engineering of the University of Porto
Gs	specific gravity
IL	Instability Locus
ISO	International Organization for Standardization
K_0	coefficient of earth pressure at rest

LabGEO	Geotechnical Laboratory of the Civil Engineering Department at FEUP
LiDAR	Laser imaging, Detection, and Ranging
M_c	slope of critical state locus in q-p' space
MG	Minas Gerais state
MPF	Federal Public Prosecutor's Office
N	intercept of normal compression line in in e-log p' space
PSD	Particle Size Distribution
SEM	Scanning Electron Microscopy
SBT	Soil Behaviour Type
SDMT	Seismic Flat Dilatometer Test
S_p	normalised undrained strength ratio
$s_{u\,pk}$	peak undrained shear strength
$s_{u\,res}$ $s_{u\,cs}$	residual undrained shear strength (q/2) on CSL after instabilization
TSF	Tailings Storage Facility
UFMG	Federal University of Minas Gerais
UFSC	Federal University of Santa Catarina
U_n	percent of undercompaction
UPC	Universitat Politècnica de Catalunya
V_P	P-wave velocity
Vs	S-wave velocity
Γ	intercept of critical state line in e-log p' space
ϕ'_{cs}	friction angle at the critical state
ϕ'_{pk}	peak friction angle
κ	slope of unloading–reloading line in e-log p' space
λ_e	slope of normal compression line / slope of critical state line in e-log p' space
σ'_v	vertical effective stress
ψ	state parameter

References

Andrade, J.E. (2009). A predictive framework for liquefaction instability. *Geotechnique*, 59(8), 673-682. https://doi.org/10.1680/geot.7.00087.

Arroyo, M., & Gens, A. (2021). *Computational analyses of dam i failure at the Corrego de Feijao Mine in Brumadinho: final report for Vale S.A.* Brasília. Retrieved in July 29, 2025, from https://www.mpf.mp.br/mg/sala-de-imprensa/docs/2021/relatorio-final-cinme-upc-1

Becker, L.B., Fabre, J.S., & Barbosa, M.C. (2023). Determination of the critical state of a silty sand iron tailings in triaxial extension tests using photographic correction. *Canadian Geotechnical Journal*, 60(4), 504-520. https://doi.org/10.1139/cgj-2021-0637.

Bedin, J., Schnaid, F., Fonseca, A., & Costa Filho, L.M. (2012). Gold tailings liquefaction under critical state soil mechanics. *Geotechnique*, 62(3), 263-267. https://doi.org/10.1680/geot.10.P.037.

Been, K., & Jefferies, M. (2011). Stress-dilatancy in very loose sand. *Canadian Geotechnical Journal*, 41(5), 972-989. https://doi.org/10.1139/t04-038.

Besenzon, D. (2024). *Liquefaction of mine tailing storage facilities: material characterization and numerical analysis* [Doctoral thesis]. Universidade do Porto. Retrieved in July 29, 2025, from https://repositorio-aberto.up.pt/handle/10216/161656

Bishop, A.W. (1967). Progressive failure – with special reference to the mechanism causing it. In *Proceedings of the Geotechnical Conf. on Shear Strength Properties of Natural Soils and Rocks* (Vol. 2, pp. 142-150), Oslo.

Boulanger, R. (2022). Nonlinear dynamic analyses involving soil liquefaction or cyclic softening. In *Proceedings of the 20th ICSMGE State of the Art and Invited Lectures* (pp. 351-379). Sydney: Australian Geomechanics Society. Retrieved in July 29, 2025, from https://www.issmge.org/publications/online-library

Boulanger, R. W., & Truman, S. P. (1996). Void redistribution in sand under post-earthquake loading. *Canadian Geotechnical Journal*, 33(5), 829-834. https://doi.org/10.1139/t96-109-329.

Carrera, A., Coop, M., & Lancellotta, R. (2011). Influence of grading on the mechanical behaviour of Stava tailings. *Geotechnique*, 61(11), 935-946. https://doi.org/10.1680/geot.9.P.009.

Castro, G. (1969). *Liquefaction of sands* (Harvard Soil Mechanics Series, No. 81). Cambridge: Harvard University.

Chapuis, R.P., & Aubertin, M. (2003). On the use of the Kozeny-Carman equation to predict the hydraulic conductivity of soils. *Canadian Geotechnical Journal*, 40(3), 616-628. https://doi.org/10.1139/t03-013.

Chapuis, R.P., & Légaré, P.P. (1992). A simple method for determining the surface area of fine aggregates and fillers in bituminous mixtures. In American Society for Testing and Materials (Ed.), *Effects of aggregates and mineral fillers on asphalt mixture performance* (ASTM Special Technical Publication, No. 1147, pp. 177-186). West Conshohocken: ASTM International.

Cho, G.-C., Dodds, J., & Santamarina, J.C. (2006). Particle shape effects on packing density, stiffness, and strength: natural and crushed sands. *Journal of Geotechnical and Geoenvironmental Engineering*, 132(5), 591-602. https://doi.org/10.1061/(ASCE)1090-0241(2006)132:5(591).

Chu, J., & Wanatowski, D. (2008). Instability conditions of loose sand in plane-strain. *Journal of Geotechnical and Geoenvironmental Engineering*, 134(1), 136-142. https://doi.org/10.1061/(ASCE)1090-0241(2008)134:1(136).

Chu, J., & Wanatowski, D. (2014). Difficulties in the determination of post-liquefaction strength for sand. *Géotechnique Letters*, 4(1), 57-61. https://doi.org/10.1680/geolett.13.00076.

Chu, J., Leong, W.K., Loke, W.L., & Wanatowski, D. (2012). Instability of loose sand under drained conditions. *Journal of Geotechnical and Geoenvironmental Engineering*, 138(2), 207-216. https://doi.org/10.1061/(ASCE)GT.1943-5606.0000574.

Chu, J., Leroueil, S., & Leong, W.K. (2003). Unstable behaviour of sand and its implication for slope stability. *Canadian Geotechnical Journal*, 40(5), 873-885. https://doi.org/10.1139/t03-039.

CIMNE. (2021). *Computational analyses of Dam I failure at the Córrego de Feijão mine in Brumadinho: final report.* Brasília. Retrieved in July 29, 2025, from http://tinyurl.com/5n8ftcay

Cordeiro, D., Molina-Gómez, F., Ferreira, C., Rios, S., & Viana da Fonseca, A. (2022). Cyclic Liquefaction Resistance of an Alluvial Natural Sand: A Comparison between Fully and Partially Saturated Condition. *Geotechnics*, 2(1), 1-13. https://doi.org/10.3390/geotechnics2010001.

Corrêa de Oliveira, S.C., Delgado, B.G., Paes, I.T., Viana da Fonseca, A.V., Pereira, E.L., & Paes, B.S.T. (2025). Influence of stress state on the expected behavior of filtered iron ore tailings for compacted stacking disposal. *Geotechnical Testing Journal*, 48(2), 166-189. https://doi.org/10.1520/GTJ20230503.

Delgado, B.G., Viana da Fonseca, A., Bittar, R.J., Besenzon, D., Molina-Gomez, F., Cordeiro, D., Mendonça, A., & Rios, S. (2025). Critical state loci of super heavy iron ore tailings from sampling in Brumadinho reservoir. *Journal of Geotechnical and Geoenvironmental Engineering*, 151(10), 04025104. https://doi.org/10.1061/JGGEFK.GTENG-13055.

Desrues, J., Chambon, R., Mokni, M., & Mazerolle, F. (1996). Void ratio evolution inside shear bands in triaxial sand specimens studied by computed tomography. *Geotechnique*, 46(3), 529-546. https://doi.org/10.1680/geot.1996.46.3.529.

Fan, J., Rowe, K.R., & Brachman, R.W.I. (2022). Compressibility and permeability of sand-silt tailings mixtures. *Canadian Geotechnical Journal*, 59(8), 1348-1357. https://doi.org/10.1139/cgj-2021-0356.

Fanni, R., Reid, D., & Fourie, A. (2022). On reliability of inferring liquefied shear strengths from simple shear testing. *Soil and Foundation*, 62(3), 101151. https://doi.org/10.1016/j.sandf.2022.101151.

Fanni, R., Reid, D., & Fourie, A. (2024). Effect of principal stress direction on the instability of sand under the constant shear drained stress path. *Geotechnique*, 74(9), 875-891. https://doi.org/10.1680/jgeot.22.00062.

Fanni, R., Reid, D., & Fourie, A. (2025). Drained and undrained behaviour of a sandy silt gold tailings under general multiaxial conditions. *Geotechnique*, 75(13), 1-20. https://doi.org/10.1680/jgeot.23.00186.

Ferreira, C., Diáz-Durán, F., Viana da Fonseca, A., & Cascante, G. (2021). New approach to concurrent Vs and Vp measurements using bender elements. *Geotechnical Testing Journal*, 44(6), 1801-1820. https://doi.org/10.1520/GTJ20200207.

Finno, R.J., & Rechenmacher, A.L. (2003). Effects of consolidation history on critical state of sand. *Journal of Geotechnical and Geoenvironmental Engineering*, 129(4), 350-360. https://doi.org/10.1061/(ASCE)1090-0241(2003)129:4(350).

Fotovvat, A., & Sadrekarimi, A. (2022). Instability of a gold mine tailings subjected to different stress paths. *Journal of Geotechnical and Geoenvironmental Engineering*, 148(5), 04022020-04022021. https://doi.org/10.1061/(ASCE)GT.1943-5606.0002780.

Fourie, A., Verdugo, R., Bjelkevik, M., Torres-Cruz, L.A., & Znidarcic, D. (2022). Geotechnics of mine tailings: a 2022 state of the art. In *Proceedings of the 20th ICSMGE-State of the Art and Invited Lectures* (pp. 121-183). Sydney: Australian Geomechanics Society.

Fourie, A.B., & Tshabalala, L. (2005). Initiation of static liquefaction and the role of K0 consolidation. *Canadian Geotechnical Journal*, 42(3), 892-906. https://doi.org/10.1139/t05-026.

Gens, A. (2019). Hydraulic fills with special focus on liquefaction. In *Proceedings of the XVII European Conference on Soil Mechanics and Geotechnical Engineering*, Reykjavik, Iceland. https://doi.org/10.32075/17ECSMGE-2019-1108.

GISTM. (2020). *Global industry standard on tailings management.* Global Tailings Review. Retrieved in July 29, 2025, from https://globaltailingsreview.org/wp-content/uploads/2020/08/global-industry-standard_EN.pdf

Guida, G., Casini, F., & Viggiani, G.M.B. (2017). Contour fractal analysis of grains. *EPJ Web of Conferences*, 140, 05008. https://doi.org/10.1051/epjconf/201714005008.

Habib, P. (1953). Influence of variation of the average principal stress on the shear strength of soils. In *Proceedings of the 3rd international Conference on Soil Mechanics and Foundation Engineering* (Vol. 1, pp. 131-136), Zurich, Switzerland. ICOSOMEF (in French).

Hight, D. (2024). The 9th Victor de Mello lecture: reflections and speculations. *Soils and Rocks*, 47(4), e2024008824. https://doi.org/10.28927/SR.2024.008824.

Hight, D., & Dias, T.G.S. (2023). Does the anisotropy of the collapse/instability surface play a role when assessing the stability of tailings dams? In *Proceedings of the 1st International Conference on Geotechnics of Tailings and Mine Waste (1-ICGTMW)* (pp. 222-235). ISSMGE. Retrieved in July 29, 2025, from https://www.issmge.org/news/proceedings-of-1st-international-conference-on-geotechnics-of-tailings-and-mine-waste

Hight, D., Grammatikopoulou, A., Dias, T., Schroeder, F., & Mello, L.G. (2023). Characterisation of tailings for dry stacks. In *Proceedings of the 1st International Conference on Geotechnics of Tailings and Mine Waste (1-ICGTMW)* (pp. 318-330), Ouro Preto, MG, Brazil. Retrieved in July 29, 2025, from https://syncandshare.lrz.de/getlink/fiJUkGWTZc4q7ZcbbD5Hz1/1-%20ICGTMW%202023_Brazil-Proceedings.pdf

Hyslip, J.P., & Vallejo, L.E. (1997). Fractal analysis of the roughness and size distribution of granular materials. *Engineering Geology*, 48(3-4), 231-244. https://doi.org/10.1016/S0013-7952(97)00046-X.

Iai, S. (2021). *Mechanism of PALU liquefaction EQ 2018: delayed flow failure.* FLIP Consortium. Retrieved in July 29, 2025, from https://www.hatti.or.id/files/2021/HATTI.pdf

Iai, S., & Tobita, T. (2022). Nonlinear dynamic analyses for evaluating seismic ground deformation: delayed flow failure. In *Proceedings of the 20th ICSMGE State of the Art and Invited Lectures* (pp. 381-401). Sydney: Australian Geomechanics Society. Retrieved in July 29, 2025, from https://www.issmge.org/publications/online-library

Ishihara, K. (1993). Liquefaction and flow failure during earthquakes. 33th Rankine Lecture. *Geotechnique*, 43(3), 351-415. https://doi.org/10.1680/geot.1993.43.3.351.

Jefferies, M., & Been, K. (2016). *Soil liquefaction: a critical state approach* (2nd ed.). Boca Raton: CRC Press.

Jefferies, M., & Shuttle, D. (2011). On the operating critical friction ratio in general stress states. *Geotechnique*, 61(8), 709-713. https://doi.org/10.1680/geot.9.T.032.

Jefferies, M., Morgenstern, N.R., Van Zyl, D.V., & Wates, J. (2019). *Report on NTSF embankment failure: Cadia valley operations for ashurst operations* (NEWCREST Technical Report). South Orange, NSW: NTSF. Retrieved in July 29, 2025, from https://s24.q4cdn.com/382246808/files/doc_news/2019/04/News-Release-1699390465077795.pdf

Jefferies, M.G., & Davies, M.P. (1993). Use of CPTu to estimate Equivalent SPT N_{60}. *Geotechnical Testing Journal*, 16(4), 458-468. https://doi.org/10.1520/GTJ10286J.

Kamai, R., & Boulanger, R.W. (2013). Simulations of a Centrifuge Test with Lateral Spreading and Void Redistribution Effects. *Journal of Geotechnical and Geoenvironmental Engineering*, 139(8), 1250-1261. https://doi.org/10.1061/(ASCE)GT.1943-5606.0000845.

Kulasingam, R., Malvick, E.J., Boulanger, R.W., & Kutter, B.L. (2004). Strength loss and localization at silt interlayers in slopes of liquefied sand. *Journal of Geotechnical and Geoenvironmental Engineering*, 130(11), 1192-1202. https://doi.org/10.1061/(ASCE)1090-0241(2004)130:11(1192).

Ladd, R. (1978). Preparing test specimens using undercompaction. *Geotechnical Testing Journal*, 1(1), 16-23. https://doi.org/10.1520/GTJ10364J.

Lade, P.V. (1992). Static instability and liquefaction of loose fine sandy slopes. *Journal of Geotechnical Engineering*, 118(1), 51-71. https://doi.org/10.1061/(ASCE)0733-9410(1992)118:1(51).

Lade, P.V. (1993). Initiation of static instability in the submarine Nerlerk Berm. *Canadian Geotechnical Journal*, 30(6), 895-904. https://doi.org/10.1139/t93-088.

Laera, A., Miranda, V.H., Azeiteiro, R.J.N., Bui, T., Brasile, S., & Brinkgreve, R.B.J. (2024). Finite element modelling of a tailings dam using the Clay And Sand Model. In *Proceedings of the XVIII ECSMGE 2024, Geotechnical Engineering Challenges to Meet Current and Emerging Needs of Society.* ISSMGE. https://doi.org/10.1201/9781003431749-319.

Li, W., & Coop, M.R. (2019). Mechanical behaviour of Panzhihua iron tailings. *Canadian Geotechnical Journal*, 56(3), 420-435. https://doi.org/10.1139/cgj-2018-0032.

Li, W., Coop, M.R., Senetakis, K., & Schnaid, F. (2018). The mechanics of a silt-sized gold tailing. *Engineering Geology*, 241, 97-108. https://doi.org/10.1016/j.enggeo.2018.05.014.

Li, X.S., & Dafalias, X.S. (2012). Anisotropic Critical State Theory: role of fabric. *Journal of Engineering Mechanics*, 138(3), 263-275. https://doi.org/10.1061/(ASCE)EM.1943-7889.0000324.

Lode, W. (1926). Experiments on the influence of the mean principal stress on the flow of the metals iron, copper and nickel. *Zeitschrift für Physik*, 36(11-12), 913-939. https://doi.org/10.1007/BF01400222.

Mánica, M., Gens, A., Vaunat, J., & Ruiz, D.F. (2018). Nonlocal plasticity modelling of strain localisation in stiff clays. *Computers and Geotechnics*, 103, 138-150. https://doi.org/10.1016/j.compgeo.2018.07.008.

Mánica, M.A., Arroyo, M., Gens, A., & Monforte, L. (2022). Application of a critical state model to the Merriespruit tailings dam failure. *Proceedings of the Institution of Civil Engineers - Geotechnical Engineering*, 175(2), 151-165. https://doi.org/10.1680/jgeen.21.00001.

Matsuoka, H., & Nakai, T. (1974). Stress-deformation and strength characteristics of soil under three different principal stresses. *Proceedings of the Japan Society of Civil Engineers*, 232(232), 59-70. https://doi.org/10.2208/jscej1969.1974.232_59.

Mishra, P.C., & Mohanty, M.K. (2020). A review of factors affecting mining operation. *World Journal of Engineering*, 17(3), 457-472. https://doi.org/10.1108/WJE-03-2019-0082.

Mitchell, J.K., & Soga, K. (2005). *Fundamentals of soil behaviour* (577 p.). New York: John Wiley & Sons

Molina-Gómez, F., & Viana da Fonseca, A. (2021). Key geomechanical properties of the historically liquefiable TP-Lisbon sand. *Soil and Foundation*, 61(3), 836-856. https://doi.org/10.1016/j.sandf.2021.03.004.

Monforte, L., Arroyo, M., & Gens, A. (2023). A relation between cone metrics and the state parameter for liquefiable soils. *Canadian Geotechnical Journal*, 60(11), 1756-1774. https://doi.org/10.1139/cgj-2022-0377.

Monforte, L., Arroyo, M., Gens, A., & Carbonell, J.M. (2018). Hydraulic conductivity from piezocone on-the-fly: a numerical evaluation. *Géotechnique Letters*, 8(4), 268-277. https://doi.org/10.1680/jgele.18.00108.

Monforte, L., Ciantia, M.O., Carbonell, J.M., Arroyo, M., & Gens, A. (2019). A stable mesh-independent approach for numerical modelling of structured soils at large strains. *Computers and Geotechnics*, 116, 103215. https://doi.org/10.1016/j.compgeo.2019.103215.

Monforte, L., Gens, A., Arroyo, M., Mánica, M., & Carbonell, J.M. (2021). Analysis of cone penetration in brittle liquefiable soils. *Computers and Geotechnics*, 134, 104123. https://doi.org/10.1016/j.compgeo.2021.104123.

Morgenstern, N.R. (2018). Geotechnical risk, regulation, and public policy: the Sixth Victor de Mello Lecture. *Soils and Rocks*, 41(2), 107-129. https://doi.org/10.28927/SR.412107.

Murthy, T.G., Loukidis, D., Carraro, J.A.H., Prezzi, M., & Salgado, R. (2007). Undrained monotonic response of clean and silty sands. *Geotechnique*, 57(3), 273-288. https://doi.org/10.1680/geot.2007.57.3.273.

Narainsamy, Y., Jacobsz, S.W., Murison, R.A., & Vermeulen, N.J. (2023). Uniqueness of the normal consolidation line for gold tailings. *Geotechnical Testing Journal*, 46(6), 1046-1065. https://doi.org/10.1520/GTJ20230325.

Nova, N. (1994). Controllability of the incremental response of soil specimens subjected to arbitrary loading programmes. *Journal of the Mechanical Behavior of Materials*, 5(2), 193-202. https://doi.org/10.1515/JMBM.1994.5.2.193.

Olson, S.M., & Stark, T.D. (2002). Liquefied strength ratio from liquefaction flow failure case histories. *Canadian Geotechnical Journal*, 39(3), 629-647. https://doi.org/10.1139/t02-001.

Pezeshki, A., & Ahmadi, M.M. (2021). In situ state of tailing silts using a numerical model of piezocone penetration test developed by Norsand model. *International Journal of Geomechanics*, 22(1), 04021264. https://doi.org/10.1061/(ASCE)GM.1943-5622.0002250.

Rabbi, A.T., Rahman, M.M., & Cameron, D.A. (2018). Undrained behaviour of silty sand and the role of isotropic and K0 consolidation. *Journal of Geotechnical and Geoenvironmental Engineering*, 144(4), 04018014. https://doi.org/10.1061/(ASCE)GT.1943-5606.0001859.

Ramirez Orbegoso, V.R. (2021). *CPTu-based state parameter evaluation in tailings* [Master's dissertation]. UNED/CEDEX, Madrid (in Spanish).

Ramos, C., Viana da Fonseca, A., & Vaunat, J. (2015). Modeling flow instability of an Algerian sand with the dilatancy rule in CASM. *Geomechanics and Engineering*, 9(6), 729-742. https://doi.org/10.12989/gae.2015.9.6.729.

Reid, D., Dickinson, S., Mital, U., Fanni, R., & Fourie, A. (2022e). On some uncertainties related to static liquefaction triggering assessments. *Proceedings of the Institution of Civil Engineers - Geotechnical Engineering*, 175(2), 181-199. https://doi.org/10.1680/jgeen.21.00054.

Reid, D., Fanni, R., & DiDonna, P. (2022b). The effect of tamping conditions on undrained shear strengths of a nonplastic sandy silt tailings. *Canadian Geotechnical Journal*, 59(6), 783-795. https://doi.org/10.1139/cgj-2020-0269.

Reid, D., Fanni, R., & Fourie, A. (2022a). Effect of tamping conditions on the shear strength of tailings. *International Journal of Geomechanics*, 22(3), 1-10. https://doi.org/10.1061/(ASCE)GM.1943-5622.0002247.

Reid, D., Fanni, R., & Fourie, A. (2022c). Assessing the undrained strength cross-anisotropy of three tailings types. *Géotechnique Letters*, 12(1), 1-7. https://doi.org/10.1680/jgele.21.00094.

Reid, D., Fourie, A., Ayala, J.L., Dickinson, S., Ochoa-Cornejo, F., Fanni, R., Garfias, J., Viana da Fonseca, A., Ghafghazi, M., Ovalle, C., Riemer, M., Rismanchian, A., & Olivera, R. (2021). Results of a critical state line testing round robin programme. *Geotechnique*, 71(7), 616-630. https://doi.org/10.1680/jgeot.19.P.373.

Reid, D., Simms, P., Sivathayalan, S., Fanni, R., & Fourie, A. (2022d). The "air dried" specimen reconstitution technique: review, refinements, and applications. In *Proceedings of the Tailings and Mine Waste*, Denver, CO, USA.

Reid, D., Urbina, F., Tiwari, B., Fanni, R., Smith, K., & Fourie, A. (2023). Effect of saturation confining pressure on accessible density and shear behaviour of sandy silt tailings. *Géotechnique Letters*, 13(2), 113-117. https://doi.org/10.1680/jgele.23.00001.

Riemer, M.F., & Seed, R.B. (1997). Factors affecting apparent position of steady-state line. *Journal of Geotechnical and Geoenvironmental Engineering*, 123(3), 281-288. https://doi.org/10.1061/(ASCE)1090-0241(1997)123:3(281).

Rios, S., Ciantia, M., Gonzalez, N., Arroyo, M., & Viana da Fonseca, A. (2016). Simplifying calibration of bonded elasto-plastic models. *Computers and Geotechnics*, 73, 100-108. https://doi.org/10.1016/j.compgeo.2015.11.019.

Robertson, P.K., & Wride, C.E. (1998). Evaluating cyclic liquefaction potential using the cone penetration test. *Canadian Geotechnical Journal*, 35(3), 442-459. https://doi.org/10.1139/t98-017.

Robertson, P.K., Melo, L., Williams, D.J., & Wilson, W. (2019). *Report of the expert panel on the technical causes of the failure of Feijão Dam I.* Retrieved in July 29, 2025, from http://www.b1technicalinvestigation.com/

Salvatore, E., Modoni, G., Andò, E., Albano, M., & Viggiani, G. (2017). Determination of the critical state of granular materials with triaxial tests. *Soil and Foundation*, 57(5), 733-744. https://doi.org/10.1016/j.sandf.2017.08.005.

Santamarina, J.C. (2003). Soil particle ate the microscale: particle forces. In *Proceedings of the Symposium on Soil Behavior and Soft Ground Construction, in honor of Charles C. Ladd* (ASCE Geotechnical Special Publication, pp. 1-23). ASCE. https://doi.org/10.1061/40659(2003)2.

Schnaid, F., Bedin, J., Viana da Fonseca, A., & Costa-Fillho, L. de M. (2013). Stiffness and strength governing the static liquefaction of tailings. *Journal of Geotechnical and Geoenvironmental Engineering*, 139(12), 2136-2144. https://doi.org/10.1061/(ASCE)GT.1943-5606.0000924.

Sento, N., Kazama, M., Uzuoka, R., Ohmura, H., & Ishimaru, M. (2004). Possibility of Postliquefaction Flow Failure due to Seepage. *Journal of Geotechnical and Geoenvironmental Engineering*, 130(7), 707–716. https://doi.org/10.1061/(ASCE)1090-0241(2004)130:7(707)

Shuttle, D., & Jefferies, M. (2016). Determining silt state from CPTu. *Geotechnical Research, ICE*, 3(3), 90-118. https://doi.org/10.1680/jgere.16.00008.

Shuttle, D., Martens, S., & Jefferies, M. (2023). Geostatic stress in oilsand tailings. Proceedings of the Institution of Civil Engineers –. *Geotechnical Engineering*, 176(3), 274-283. https://doi.org/10.1680/jgeen.21.00114.

Silva, J.P., Rissoli, A.L.C., Cacciari, P.P., Viana da Fonseca, A.J.P., Scheuermann Filho, H.C., Wagner, A.C., Carvalho, J.V.A., Festugato, L., & Consoli, N.C. (2024). Triaxial testing response of compacted iron ore tailings considering a broad spectrum of confining pressures. *Soil and Foundation*, 64(2), 10143861. https://doi.org/10.1016/j.sandf.2024.101438.

Smith, K., Fanni, R., Chapman, P., & Reid, D. (2019). Critical state testing of tailings: comparison between various tailings and implications for design. In *Proceedings of the Tailings and Mine Waste* (pp. 1183-1195), Vancouver, BC.

Soares, M., & Viana da Fonseca, A. (2016). Factors affecting steady state locus in triaxial tests. *Geotechnical Testing Journal*, 39(6), 1056-1078. https://doi.org/10.1520/GTJ20150228.

Soares, M., Viana da Fonseca, A., Ferreira, C., & Rios, S. (2023). Static liquefaction assessment combining shear wave velocity, peak strength and soil grading. *Applied Sciences*, 13(15), 8580. https://doi.org/10.3390/app13158580.

Vaid, Y. P., & Eliadorani, A. (2000). Undrained and drained (?) stress-strain response. *Canadian Geotechnical Journal*, 37(5), 1126-1130. https://doi.org/10.1139/t00-036

Vaid, Y.P., & Eliadorani, A. (1998). Instability and liquefaction of granular soils under undrained and partially drained states. *Canadian Geotechnical Journal*, 35(6), 1053-1062. https://doi.org/10.1139/t98-061.

Van Eekelen, H.A.M. (1980). Isotropic yield surfaces in three dimensions for use in soil mechanics. *International Journal for Numerical and Analytical Methods in Geomechanics*, 4(1), 89-101. https://doi.org/10.1002/nag.1610040107.

Verdugo, R., & Ishihara, K. (1996). The steady state of sandy soils. *Soil and Foundation*, 36(2), 81-91. https://doi.org/10.3208/sandf.36.2_81.

Viana da Fonseca, A. (2013). Application of in situ testing in tailing dams, emphasis on liquefaction: Case-history. In R. Q. Coutinho & P. W. Mayne (Eds), *Geotechnical and Geophysical Site Characterization 4* (pp. 181–203). Taylor & Francis Group.

Viana da Fonseca, A., Besenzon, D., & Molina-Gómez, F. (2022). Flow liquefaction susceptibility of pond filled iron ore mining tailings from CPTu data: a comparison between state parameter and yield-stress-ratio approaches. In *Proceedings of the 20th ICSMGE* (pp. 4423-4428). Sydney: Australian Geomechanics Society. Retrieved in July 29, 2025, from https://www.issmge.org/publications/online-library

Viana da Fonseca, A., Coop, M.R., Fahey, M., & Consoli, N. (2011). The interpretation of conventional and non-conventional laboratory tests for challenging geotechnical problems. 'Deformation Characteristics of Geomaterials', Vol. 1, pp. 84-119. IOS Press, Amsterdam. https://doi.org/10.3233/978-1-60750-822-9-84.

Viana da Fonseca, A., Cordeiro, D., & Molina-Gómez, F. (2021b). Recommended procedures to assess critical state locus from triaxial tests in cohesionless remoulded samples. *Geotechnics*, 1(1), 95-127. https://doi.org/10.3390/geotechnics1010006.

Viana da Fonseca, A., Ferreira, C., & Fahey, M. (2009). A framework interpreting bender element tests, combining time-domain and frequency-domain methods. *Geotechnical Testing Journal*, 32(2), 91-107. https://doi.org/10.1520/GTJ100974.

Viana da Fonseca, A., Ferreira, C., Ramos, C., & Molina-Gómez, F. (2019). The geotechnical test site in the greater Lisbon area for liquefaction characterisation and sample quality control of cohesionless soils. *AIMS Geosciences*, 5(2), 325-343. https://doi.org/10.3934/geosci.2019.2.325.

Viana da Fonseca, A., Fonseca, A., & Oliveira, S. (2021). Fatores de segurança determinísticos em avaliação de estabilidade de barragens de rejeitos: uma reflexão. *Geotecnia*, 151(151), 53-76. https://doi.org/10.24849/j.geot.2021.151.04.

Viana da Fonseca, A., Molina-Gomez, F., Besenzon, D., & Coelho, D. (2023). The influence of stress induced anisotropy in undrained yield and ultimate shear strengths in brittle loose deposited silts. *E3S Wes of Conferences*, 544, 14006. https://doi.org/10.1051/e3sconf/202454414006.

Wagner, A.C., de Sousa Silva, J.P., de Azambuja Carvalho, J.V., Cezar Rissoli, A.L., Cacciari, P.P., Chaves, H.M., Scheuermann Filho, H.C., & Consoli, N.C. (2023). Mechanical behaviour of iron ore tailings under standard compression and extension triaxial stress paths. *Journal of Rock Mechanics and Geotechnical Engineering*, 15(7), 1883-1894. https://doi.org/10.1016/j.jrmge.2022.11.013.

Yamamuro, J.A., & Lade, P.V. (1996). Drained sand behaviour in axisymmetric tests at high pressures. *Journal of Geotechnical Engineering*, 122(2), 109-119. https://doi.org/10.1061/(ASCE)0733-9410(1996)122:2(109).

Yang, J. (2002). Liquefaction resistance of sand in relation to P-wave velocity. *Geotechnique*, 52(4), 295-298. https://doi.org/10.1680/geot.2002.52.4.295.

Yang, J., & Luo, X.D. (2015). Exploring the relationship between critical state and particle shape for granular materials. *Journal of the Mechanics and Physics of Solids*, 84, 196-213. https://doi.org/10.1016/j.jmps.2015.08.001.

Yoshimine, M., Nishizaki, H., Amano, K., & Hosono, Y. (2006). Flow Deformation of Liquefied Sand Under Constant Shear Load And Its Application To Analysis Of Flow Slide Of Infinite Slope. *Soil Dynamics and Earthquake Engineering*, 26(2-4), 253-264. https://doi.org/10.1016/j.soildyn.2005.02.016.

YouTube. (2015). *Brazil's mining catastrophe.* Retrieved in July 29, 2025, from www.youtube.com/watch?v=_HKnOVLpTZQ

YouTube. (2016). *Bento Rodrigues mine disaster.* Retrieved in July 29, 2025, from www.youtube.com/watch?v=k0PWRiEWMTY

YouTube. (2018). *A 2015 dam break in Brazil that covered villages in toxic mud.* Retrieved in July 29, 2025, from www.youtube.com/watch?v=MjcJKag_6b0

YouTube. (2019). *Brumadinho (Brasil) dam collapse: during and after collapse footages.* Retrieved in July 29, 2025, from www.youtube.com/watch?v=lCoTcIMQ27k

Yu, H.S., Khong, C., Wang, J., & Zhang, G. (2005). Experimental evaluation and extension of a simple critical state model for sand. *Granular Matter*, 7(4), 213-225. https://doi.org/10.1007/s10035-005-0209-y.